

# Threshold dynamics and bifurcation of a state-dependent feedback nonlinear control SIR model<sup>☆</sup>

Tianyu Cheng<sup>a</sup>, Sanyi Tang<sup>a,\*</sup>, Robert A. Cheke<sup>b</sup>

<sup>a</sup>*School of Mathematics and Information Science, Shaanxi Normal University, Xi'an, 710119, P.R. China*

<sup>b</sup>*Natural Resources Institute, University of Greenwich at Medway, Central Avenue, Chatham Maritime, Chatham, Kent, ME4 4TB, UK*

---

## Abstract

A classic SIR model with nonlinear state-dependent feedback control is proposed and investigated in which integrated control measures, including vaccination, treatment and isolation, are applied once the number of the susceptible population reaches a threshold level. The interventions are density dependent due to limitations on the availability of resources. The existence and global stability of the disease free periodic solution (DFPS) are addressed, and the threshold condition is provided which can be used to define the control reproduction number  $R_c$  for the model with state-dependent feedback control. The DFPS may also be globally stable even if the basic reproduction number  $R_0$  of the SIR model is larger than one. To show that the threshold dynamics are determined by the  $R_c$ , we employ bifurcation theories of the discrete one-parameter family of maps, which are determined by the Poincaré map of the proposed model, and the main results indicate that under certain conditions a stable or unstable interior periodic solution could be generated through transcritical, pitchfork and backward bifurcations. A biphasic vaccination rate (or threshold level) could result in an inverted U-shape (or U-shape) curve which reveals some important issues related to disease control and vaccine design in bioengineering including vaccine coverage, efficiency and vaccine production. Moreover, the nonlinear

---

<sup>☆</sup>Fully documented templates are available in the elsarticle package on CTAN.

\*Corresponding author

Email address: [sytang@snnu.edu.cn](mailto:sytang@snnu.edu.cn) & [sanyitang219@hotmail.com](mailto:sanyitang219@hotmail.com) (Sanyi Tang)

state-dependent feedback control could result in novel dynamics including various bifurcations.

*Keywords:* SIR model, Disease free periodic solution, Control reproduction number, Poincaré map, Transcritical and pitchfork bifurcations, Backward bifurcation

*2010 MSC:* 34A37, 34C23, 92B05, 93B52

---

## 1. Introduction

Although outbreaks of traditional infectious diseases have been prevented or controlled in the recent past, outbreaks of emerging infectious diseases such as SARS, H1N1 influenza, Dengue fever and Ebola, have provided new threats and challenges. Comprehensive prevention and control strategies, including quarantine, isolation, vaccination and treatment, are widely used to reduce the spread of such infectious diseases [1, 2, 3, 4] but evaluating the effectiveness of the mitigating measures is also crucial. To address this problem, mathematical models can play key roles by modelling the control tactics and revealing their effectiveness.

Recently, several mathematical models have been proposed to investigate integrated control impacts [3, 4]. Existing approaches to modelling the impact of integrated control measures have focused on how to include the tactics into models and address their effects on the dynamics and disease control. There are two types of important models to be chosen according to how the control measures are implemented: continuous models with a continuous control strategy [1, 2, 3, 4] and continuous models with a discrete (pulse) control strategy [5, 6, 7]. The two types of models with the continuous vaccination and pulsed vaccination were compared with each other in epidemiological models [5]. The results of that study were confirmed by the pulse vaccination campaigns against measles performed in 1994 in the UK, which revealed that a pulse vaccination strategy had a dramatic impact on the development of the epidemic.

The pulse vaccination strategy was applied at a fixed period  $T$ , i.e. at dis-

crete times  $nT$  ( $n = 1, 2, \dots$ ) a proportion of the susceptible population was  
25 vaccinated and removed into the recovered or removed or vaccinated class instan-  
taneously, which action can be formulated by impulsive differential equations  
with a fixed moment [8, 9, 10, 11, 12, 13, 14, 7]. The dynamical behaviour,  
including the existence and local stability of the disease free periodic solution  
has been investigated, which revealed that pulse vaccination was always capa-  
30 ble of eradicating the diseases, usually doing better than continuous vaccination.  
Numerical bifurcation analyses depict that pulse vaccination can lead to very  
complex dynamics including chaotic behaviour. In addition, this type of mod-  
elling has been widely used for cancer treatment [15, 16, 17, 18, 19] and HIV  
control [20, 21].

35 However, one common assumption of all the above models is that, regard-  
less of the size of the susceptible population, the pulse vaccination control is  
implemented at fixed periods. The obvious conclusion is that as long as the  
pulse period is small enough, the disease can be controlled and eradicated even-  
tually. Moreover, from a mathematical point of view, fixed moment control  
40 will result in a non-autonomous system which poses a considerable challenge to  
theoretical analysis. In particular, it is difficult to define the control reproduc-  
tion number  $R_c$  and investigate the threshold dynamics of the proposed models  
[8, 11, 12, 13, 14, 7]. In order to overcome the above shortcomings, a different  
modelling method is proposed in the present paper, i.e. we consider whether  
45 or not the integrated control strategy is implemented depends on the number  
in the susceptible population rather than having it applied at a fixed period.  
This can be modelled by state-dependent impulsive differential equations (so  
called impulsive semi-dynamical systems) [22, 23, 24, 25, 26, 27, 28, 29, 30, 31].  
Recently, impulsive semi-dynamical systems have been widely used to model  
50 biological systems with threshold control strategies, such as biological resource  
and pest management programmes, and chemostat cultures in ecological sys-  
tems [32, 33, 34, 27, 28, 35, 36, 37].

Therefore, in the present paper we extend the classic SIR infectious model  
with a state dependent feedback control strategy. In particular, although state

55 dependent impulsive models triggered by the infectious population size are reasonable, such models do not have a feasible disease-free equilibrium nor can the disease be completely eradicated, so far as mathematical and epidemiological points of view are concerned. Therefore, the time when vaccination strategies are implemented should, perhaps, be dependent on the level of susceptibility instead of disease infection rates. So, in this study, we propose a state-dependent  
60 impulsive model describing susceptible population-triggered vaccination and isolation incorporating continuous treatment for the patients. We assume that there exists a threshold level  $S_v$  for the susceptible population such that integrated control measures (pulse vaccination, treatment or isolation strategies) are implemented once the susceptible population number reaches  $S_v$ . Furthermore,  
65 the numbers in the susceptible and infected populations that are vaccinated and treated (or isolated), respectively, depend on their densities. This indicates that the pulse controls are nonlinear due to limitations on the amount of resources available. Note that linear pulse control has been addressed in the  
70 reference [38], from which the existence and stability of a disease free periodic solution were studied, and the bifurcations related to the key parameters were also investigated.

The main purpose of this study is to develop analytical techniques and provide a comprehensive qualitative analysis of the global dynamics by analyzing a  
75 planar impulsive SIR semi-dynamic model, and to address the effects of nonlinear feedback pulse control on the dynamics including the bifurcations in comparison with the results obtained in [38]. To achieve these aims, the existence and global stability of the disease free periodic solution (DFPS), which corresponds to the disease free equilibrium, are first addressed. The control reproduction  
80 number  $R_c$  for the model with state-dependent feedback control can be defined by the Floquet multiplier which ensures the local stability of the DFPS. It is interesting that the DFPS may also be globally stable even if the basic reproduction number  $R_0$  of the classic SIR model is larger than one. In order to depict the threshold dynamics determined by the  $R_c$ , we employ the bifurcation  
85 theories of the discrete one-parameter family of maps, which is determined by

the Poincaré map of the planar impulsive SIR semi-dynamic model. We choose the maximal vaccination rate, maximal treatment rate or isolation rate, threshold level  $S_v$  and birth rate of the susceptible population to reveal transcritical and pitchfork bifurcations, which can depict the threshold dynamics completely.

90 The main bifurcation results indicate that under certain conditions a stable or an unstable interior periodic solution could be generated through transcritical and pitchfork bifurcations. In particular, the stable DFPS and the interior equilibrium of the SIR model can coexist once an unstable interior periodic solution has bifurcated ( $R_c < 1 < R_0$  here), i.e. backward bifurcation occurs. Further-

95 more, we discuss the corresponding biological implications related to the disease control and vaccine design in bioengineering.

## 2. The model

Let  $S(t)$ ,  $I(t)$  and  $R(t)$  be the densities of susceptible, infected and removed parts of the population at time  $t$ , respectively, and then  $N(t) = S(t) + I(t) + R(t)$  denotes the total population. Without loss of generality, we may assume that

100 the total population  $N(t)$  is a constant or tends to a constant as  $t$  approaches infinity. Therefore, for the classical SIR model we only need to consider the following two dimensional system:

$$\begin{cases} \frac{dS(t)}{dt} = \Lambda - \beta SI - \delta S, \\ \frac{dI(t)}{dt} = \beta SI - qI, \end{cases} \quad (1)$$

where  $\Lambda$  denotes the birth rate,  $\delta$  is the death rate,  $\gamma$  represents the recovery rate with  $q = \gamma + \delta$ , and  $\beta$  denotes the transmission rate.

105

It is easy to know that the region

$$D = \{(S, I) | S \geq 0, I \geq 0, S + I \leq \Lambda/\delta\}$$

is an invariant set of model (1). Solving  $\Lambda - \beta SI - \delta S = 0$  and  $\beta SI - qI = 0$  with respect to  $I$  yields two isolines as follows:

$$l_1 : S = \frac{q}{\beta}, \quad l_2 : I = \frac{-\delta S + \Lambda}{\beta S} \doteq h(S),$$

where  $\doteq$  means definition in this paper.

By defining  $R_0 = \frac{\Lambda\beta}{\delta q}$ , we have the following results for model (1) which are useful for the coming qualitative analyses [38].

**Lemma 1.** *If  $R_0 \leq 1$  then model (1) has a disease free equilibrium  $(K, 0)$  with  $K = \frac{\Lambda}{\delta}$  which is a globally stable node; If  $R_0 > 1$  then there exists a unique interior equilibrium  $(S^*, I^*)$  with  $S^* = \frac{q}{\beta}$ ,  $I^* = \frac{\Lambda\beta - \delta q}{\beta q}$ , which is a globally stable node (when  $\Delta \geq 0$ ) or focus (when  $\Delta < 0$ ). Further, if  $R_0 \in (1, R_1] \cup [R_2, +\infty)$  then the unique endemic equilibrium  $P^*(S^*, I^*)$  is a globally stable node; If  $R_0 \in (R_1, R_2)$  then  $P^*(S^*, I^*)$  is a globally stable focus, where  $\Delta = \delta^2 R_0^2 - 4\delta q R_0 + 4\delta q$ ,  $R_1 = \frac{2(\delta + \gamma - \sqrt{\gamma(\delta + \gamma)})}{\delta}$ ,  $R_2 = \frac{2(\delta + \gamma + \sqrt{\gamma(\delta + \gamma)})}{\delta}$  and  $R_2 > 2 > R_1 > 1$ .*

### 2.1. The SIR model with state-dependent feedback nonlinear control

In order to consider the saturation phenomenon resulting from the limited resources, we fix the two impulsive functions to be nonlinear continuously differentiable functions  $\left[1 - \frac{\eta_1 S(t)}{S(t) + h_1}\right] S(t)$  and  $\left[1 - \frac{\eta_2 I(t)}{I(t) + h_2}\right] I(t)$ . Here  $1 > \eta_1 \geq 0$  represents the maximal vaccination rate and  $h_1 \geq 0$  denotes the half saturation constant for the susceptible population.  $1 > \eta_2 \geq 0$  represents the maximal treatment or isolation rate and  $h_2 \geq 0$  denotes the half saturation constant for the infected population. We assume that the initial density of the susceptible population is less than the threshold vaccination level  $S_v$  and the integrated mitigating measures including vaccination, treatment and isolation are conducted once the density of the susceptible population reaches the threshold  $S_v$ , when the densities of both the susceptible and infected populations are updated to  $\left[1 - \frac{\eta_1 S_v}{S_v + h_1}\right] S_v$  and  $\left[1 - \frac{\eta_2 I(t)}{I(t) + h_2}\right] I(t)$ , respectively.

Based on the above, we propose the following SIR model with state-dependent

$$\left\{ \begin{array}{l} \frac{dS(t)}{dt} = \Lambda - \beta SI - \delta S, \\ \frac{dI(t)}{dt} = \beta SI - \gamma I - \delta I, \end{array} \right\} \quad S(t) < S_v, \quad (2)$$

$$\left\{ \begin{array}{l} S(t^+) = \left[1 - \frac{\eta_1 S(t)}{S(t)+h_1}\right] S(t), \\ I(t^+) = \left[1 - \frac{\eta_2 I(t)}{I(t)+h_2}\right] I(t), \end{array} \right\} \quad S(t) = S_v.$$

Denoting the following functions  $B_1(S) = -\frac{\eta_1 S^2}{S+h_1}$ ,  $B_2(I) = -\frac{\eta_2 I^2}{I+h_2}$  and  $f(I) = I + B_2(I) < I$ , then by simple calculations we have

$$B_2'(I) = -\frac{\eta_2 I(I+2h_2)}{(I+h_2)^2}, \quad f'(I) = \frac{(1-\eta_2)I^2 + 2h_2(1-\eta_2)I + h_2^2}{(I+h_2)^2}.$$

It is easy to see that  $f'(I) > 0$  for all  $I > 0$ , which indicates that  $f(I)$  is a monotonically increasing function.

To prepare for the following definition and analysis of the Poincaré map, we first define two straight lines as follows:

$$l_3 : S = S_v \quad \text{and} \quad l_4 : S = S_u$$

with  $S_u \doteq \left[1 - \frac{\eta_1 S_v}{S_v+h_1}\right] S_v$ . Given that  $0 < S_v < K$  and substituting  $S = S_v$  into  $h(S)$ , yields the intersection point of two lines  $l_2$  and  $l_3$ , denoted by  $Q_{S_v} = (S_v, I_{S_v})$  with

$$I_{S_v} = \frac{\Lambda - \delta S_v}{\beta S_v}.$$

$$I_{S_v} = \frac{\Lambda - \delta S_v}{\beta S_v}.$$

Similarly, we can get the intersection point of the two lines  $l_2$  and  $l_4$ , denoted by  $Q_{S_u}^+ = (S_u, I_{S_u})$  with  $I_{S_u} = \frac{\Lambda - \delta S_u}{\beta S_u}$ .

## 135 2.2. Existence and stability of the DFPS

Let  $I(t) = 0$  and consider the following subsystem

$$\left\{ \begin{array}{l} \frac{dS(t)}{dt} = \Lambda - \delta S, \quad S(t) < S_v, \\ S(t^+) = \left[1 - \frac{\eta_1 S(t)}{S(t)+h_1}\right] S(t), \quad S(t) = S_v. \end{array} \right. \quad (3)$$

Solving equation (3) with initial value  $S_0 = S(0^+) = S_u$  we can obtain the following periodic solution

$$S^T(t) = K - (K - S_u) \exp(-\delta t)$$

with period

$$T = \int_{S_u}^{S_v} \frac{1}{\Lambda - \delta S} dS = -\frac{1}{\delta} \ln \left( \frac{K - S_v}{K - S_u} \right).$$

This indicates that a DFPS exists for model (2), denoted by  $(S^T(t), 0)$ , and for its stability we have the following main results

**Theorem 1.** *If  $R_0 \leq 1$  then the DFPS  $(S^T(t), 0)$  of model (2) is globally asymptotically stable.*

**Proof 1.** *It follows from Lemma A.1 in the Appendix that we have  $\phi(S, I) = S - S_v$ ,  $\sigma_1(S, I) = -\frac{\eta_1 S^2}{S+h_1}$  and  $\sigma_2(S, I) = -\frac{\eta_2 I^2}{I+h_2}$ . By simple calculation one has*

$$\frac{\partial \sigma_2}{\partial I} \frac{\partial \phi}{\partial S} - \frac{\partial \sigma_2}{\partial S} \frac{\partial \phi}{\partial I} + \frac{\partial \phi}{\partial S} = 1 - \frac{\eta_2 I(I+2h_2)}{(h_2+I)^2}, \quad \frac{\partial \sigma_1}{\partial S} \frac{\partial \phi}{\partial I} - \frac{\partial \sigma_1}{\partial I} \frac{\partial \phi}{\partial S} + \frac{\partial \phi}{\partial I} = 0$$

and  $\Delta_1 = (1 - \frac{\eta_2 I(I+2h_2)}{(h_2+I)^2})P_+/P = (1 - \frac{\eta_2 I(I+2h_2)}{(h_2+I)^2}) \frac{K-S_u}{K-S_v}$ . Moreover,

$$\begin{aligned} \int_0^T \left( \frac{\partial P}{\partial S} + \frac{\partial Q}{\partial I} \right) dt &= \int_0^T (\beta S^T(t) - \delta - q) dt \\ &\doteq J_1 + J_2 + J_3, \end{aligned}$$

where

$$J_1 = -\delta T = \ln \left( \frac{K - S_v}{K - S_u} \right),$$

$$J_2 = \int_0^T \beta S^T(t) dt = \int_{S_u}^{S_v} \frac{\beta S}{\Lambda - \delta S} dS = \frac{\beta}{\delta} \left( K \ln \frac{K - S_u}{K - S_v} + S_u - S_v \right)$$

and

$$J_3 = -qT = \int_{S_u}^{S_v} \frac{-q}{\Lambda - \delta S} dS = \frac{q}{\delta} \ln \left( \frac{K - S_v}{K - S_u} \right).$$

In particular, if  $h_2 = 0$  then we have  $B'_2(0) = -\eta_2$  with  $\Delta_1 = (1 - \eta_2) \frac{K-S_u}{K-S_v}$ ; If  $h_2 \neq 0$  then  $B'_2(0) = 0$  with  $\Delta_1 = \frac{K-S_u}{K-S_v}$ . Therefore, we have  $\mu_2 = \exp(J_2 + J_3) > 0$  for  $h_2 \neq 0$ , and  $\mu_2 = (1 - \eta_2) \exp(J_2 + J_3) > 0$  for  $h_2 = 0$ .



It follows from the monotonicity of the function  $\omega_1(x) \doteq \ln(1-x) + x$  and  
 145 inequalities  $0 < S_u < S_v \leq K$  that we have  $J_2 > 0$ . Obviously,  $J_3 < 0$  holds,  
 and we have

$$\begin{aligned}
 J_2 + J_3 &= \int_{S_u}^{S_v} \frac{\beta S - q}{\Lambda - \delta S} dS = -\frac{\beta}{\delta}(S_v - S_u) + \frac{1}{\delta}(\beta K - q) \ln \left( \frac{K - S_u}{K - S_v} \right) \\
 &= \frac{q}{\delta} \left[ (R_0 - 1) \ln \left( \frac{K - S_u}{K - S_v} \right) - \frac{\beta}{q}(S_v - S_u) \right] \\
 &= \frac{q}{\delta} \left[ (R_0 - 1) \ln \left( \frac{R_0 - \frac{S_u}{S^*}}{R_0 - \frac{S_v}{S^*}} \right) - \left( \frac{S_v}{S^*} - \frac{S_u}{S^*} \right) \right] \\
 &< \frac{q(R_0 - 1)}{\delta} \ln \left( \frac{K - S_u}{K - S_v} \right),
 \end{aligned} \tag{4}$$

which indicates that if  $R_0 \leq 1$  then we have  $\mu_2 < 1$ , and consequently the DFPS  
 is locally stable.

For the global stability, we only need to show that the DFPS  $(S^T(t), 0)$  is  
 150 globally attractive. To do this, we assume, without loss of generality, that the  
 impulsive point series  $I_k^+$  of any solution starting from the  $l_4$  with  $I_k^+ \in [0, I_{S_u}]$   
 for all  $k \geq 0$ . It follows from  $R_0 \leq 1$  and  $S_v < K$  that we have  $\frac{dI}{dt} < 0$  for  
 $S \leq S_v$ . Thus, it follows from the properties of the function  $f(I)$  that  $\{I_k^+\}$   
 is a strictly decreasing sequence with  $\lim_{k \rightarrow +\infty} I_k^+ = I_0$ , as shown in Fig.1(B).  
 155 Moreover, we claim that  $I_0 = 0$  must hold, otherwise it contradicts  $\frac{dI}{dt} < 0$  for  
 $S \leq S_v$ . Therefore, the DFPS  $(S^T(t), 0)$  is globally attractive. This completes  
 the proof.

**Remark 1.** It follows from the proof of Theorem 1 that  $R_0 \leq 1$  implies  $\mu_2 < 1$ ,  
 which means that the non-existence of the interior equilibrium for uncontrolled  
 system (1) indicates the existence and global stability of the DFPS  $(S^T(t), 0)$  of  
 controlled system (2). Naturally, we can define the multiplier  $\mu_2$  as the control  
 reproduction number, denoted by  $R_c$  with

$$R_c = \exp(J_2 + J_3) > 0 \text{ for } h_2 \neq 0, \text{ and } R_c = (1 - \eta_2) \exp(J_2 + J_3) > 0 \text{ for } h_2 = 0,$$

and interesting questions that arise are as follows: (a) whether or not the thresh-  
 old dynamical behaviour of model (2) is determined by  $R_c$ ? (b) how to determine  
 160 the dynamics of model (2) when  $\mu_2 = R_c < 1 < R_0$  or  $R_c > 1$ ?

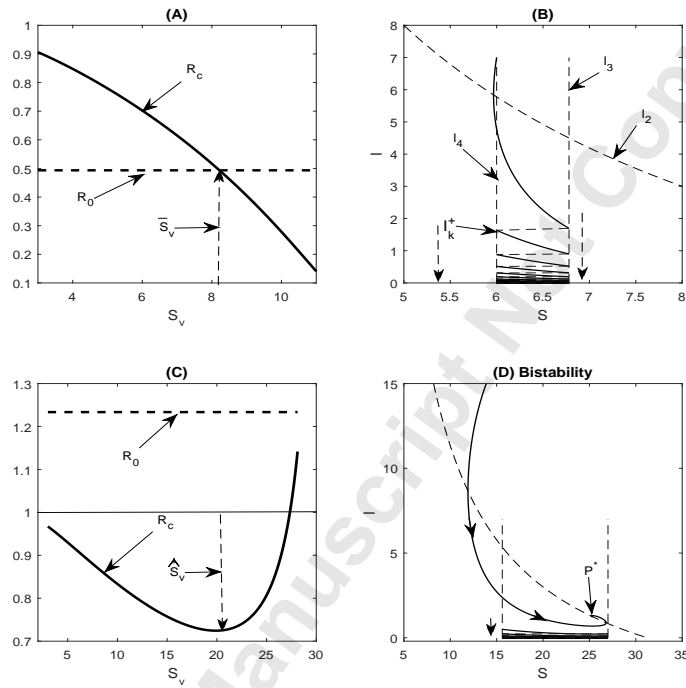


Figure 1: The relationship between  $R_0$  and  $R_c$  in (A) and (C), and the global stability of the DFPS and bi-stability in (B) and (D). The parameter values are as follows:  $\Lambda = 1$  in (A) and (B) with  $S_v = 6.78$  and  $\eta_1 = 0.2$ ,  $\Lambda = 2.5$  in (C) and (D) with  $S_v = 27$  and  $\eta_1 = 0.5$ . The other parameter values are as follows:  $\beta = 0.015$ ,  $\delta = 0.08$ ,  $\gamma = 0.3$ ,  $h_1 = 5$ ,  $\eta_2 = 0.1$ ,  $h_2 = 3$ .

**Remark 2.** *The relationships between  $R_0$  and  $R_c$  have been shown in Fig.1(A) and (C) for  $R_0 < 1$  and  $R_0 > 1$ , respectively. Although  $R_0 \leq 1$  indicates  $R_c < 1$  (Fig.1(A)), we found that  $R_c$  could be larger than  $R_0$  once the threshold  $S_v$  is less than the critical value  $\bar{S}_v$ . This confirms that the implementation of*  
165 *integrated control measures is not conducive to the elimination of the disease when the control threshold level  $S_v$  is less than the critical value  $\bar{S}_v$ . While for  $R_0 > 1$ , the relations between the  $R_0$  and  $R_c$  could be more complex which will be addressed in the Discussion section. It is interesting to note that the reproduction number  $R_c$  is a non-monotonic function of  $S_v$ , and there exists a critical*  
170 *value, denoted by  $\hat{S}_v$ , such that  $R_c$  reaches its minimal value. This clarifies that the correct selection of the threshold level  $S_v$  is beneficial to the control of the disease. However, the DFPS and interior equilibrium  $P^*$  could coexist and bi-stability occurs in this case, which reveals some interesting dynamics related to the transcritical and backward bifurcations for model (2) (see more details in*  
175 *the coming sections), as shown in Fig.1(D).*

### 3. Poincaré map and dynamics of model (2) for $R_0 \leq 1$

Although the global dynamics of model (2) for  $R_0 \leq 1$  have been given in Theorem 1, in order to address the threshold dynamics related to  $R_c$  and all possible dynamics for  $R_0 > 1$  we need to develop new methods, described below.

#### 3.1. The definition of the Poincaré map

Denote  $V_{S_v} = \{(S, I) | S = S_v, I \geq 0\}$  and  $V_{S_u} = \{(S, I) | S = S_u, I \geq 0\}$ . We choose the section  $V_{S_u}$  as a Poincaré section. Assume that the point  $P_k^+ = (S_u, I_k^+)$  lies in the section  $V_{S_u}$ , and the trajectory initiating from  $P_k^+$  will reach the section  $V_{S_v}$  in a finite time, denote the intersection point as  $P_{k+1} =$   
185  $(S_v, I_{k+1})$ , where  $I_{k+1}$  is determined by  $I_k^+$ . Without loss of generality, we can assume that  $I_{k+1} \doteq \mathcal{P}(I_k^+)$  is determined by the trajectory of model (1). A single state dependent feedback control action is implemented at point  $P_{k+1}$  such that it jumps to point  $P_{k+1}^+ = (S_u, I_{k+1}^+)$  with  $I_{k+1}^+ = I_{k+1} + B_2(I_{k+1})$  on

$V_{S_u}$ . Therefore, we can define the Poincaré map  $P_M$  as

$$I_{k+1}^+ = \mathcal{P}(I_k^+) + B_2(I_{k+1}) \doteq P_M(I_k^+). \quad (5)$$

Now we define the impulsive set  $M$  as

$$\mathcal{M} = \{(S, I) \in R_+^2 | S = S_v, 0 \leq I \leq I_M\},$$

which is a closed subset of  $R_+^2$ , where  $I_M = \mathcal{P}(I_{S_u})$  for  $R_0 \leq 1$ . Define the continuous function  $F : (S_v, I) \in \mathcal{M} \rightarrow (S^+, I^+) = (S_u, f(I)) \in R_+^2$ , where  $f(I)$  is continuous and increasing in  $[0, I_M]$ . Thus, the phase set can be defined as follows:

$$\mathcal{N} = F(\mathcal{M}) = \{(S^+, I^+) \in R_+^2 | S^+ = S_u, 0 \leq I^+ \leq f(I_M)\}.$$

190 Meanwhile, the Poincaré map  $P_M$  can be determined by the impulsive points in the phase set according to the phase portrait. To show this, we define a scalar differential equation in phase space

$$\begin{cases} \frac{dI}{dS} = \frac{I[-q + \beta S]}{\Lambda - \delta S - \beta SI} \doteq G(S, I), \\ I(S_u) = I_0^+. \end{cases} \quad (6)$$

For model (6), we only focus on the region

195

$$\Omega = \{(S, I) | S > 0, I > 0, I < h(S)\}, \quad (7)$$

in which the function  $G(S, I)$  is continuously differentiable. Further we denote  $I_0^+ \doteq Y$  with  $Y \in \mathcal{N}$  and  $Y < I_{S_u}$ , i.e. we have  $(S_0^+, Y) \in \Omega$ . Then we have

$$I(S) = I(S; S_u, Y) = I(S, Y), S_u \leq S \leq S_v$$

and

$$I(S, Y) = Y + \int_{S_u}^S G(s, I(s, Y)) ds.$$

Thus,  $P_M$  takes the form in  $\Omega$

$$P_M(I_k^+) = I_{k+1}^+ = I(S_v, I_k^+) + B_2(I(S_v, I_k^+)),$$

$$P_M(Y) = I(S_v, Y) + B_2(I(S_v, Y)) = f(I(S_v, Y)).$$

**Theorem 2.** For  $R_0 \leq 1$ , the Poincaré map  $P_M$  of model (2) satisfies the following properties:

- a) the domain and range of  $P_M$  are  $[0, I_{S_u}] \cup (I_{S_u}, +\infty)$  and  $[0, P_M(I_{S_u})]$  respectively. Moreover,  $P_M$  is continuous and concave on the interval  $[0, I_{S_u}]$ .
- 200 b)  $P_M$  has a unique fixed point  $I = 0$  which is globally stable, i.e. the DFPS of model (2) is globally stable.

**Proof 2.** By simple calculations we have

$$\frac{\partial G(S, I)}{\partial I} = \frac{(\Lambda - \delta S)(-q + \beta S)}{(\Lambda - \delta S - \beta SI)^2}, \quad \frac{\partial^2 G(S, I)}{\partial I^2} = \frac{2(\Lambda - \beta S)\beta S(-q + \beta S)}{(\Lambda - \delta S - \beta SI)^3}.$$

It follows from  $S_u \leq S_v < K$  and  $R_0 \leq 1$  that  $\Lambda - \delta S > 0$  and  $-q + \beta S < 0$  for  $S \leq S_v$ , while  $\Lambda - \delta S - \beta SI > 0$  for  $I < I_{S_u}$  and  $\Lambda - \delta S - \beta SI < 0$  for  $I > I_{S_u}$ . All these results confirm that  $\frac{\partial G(S, I)}{\partial I} < 0$  and  $\frac{\partial^2 G(S, I)}{\partial I^2} < 0$  for all  $I < I_{S_u}$ .

According to the theorem of Cauchy and Lipschitz with parameters on the scalar differential equation we have

$$\frac{\partial I(S, Y)}{\partial Y} = \exp\left(\int_{S_u}^S \frac{\partial}{\partial I} G(s, I(s, Y)) ds\right) > 0$$

205 and

$$\frac{\partial^2 I(S, Y)}{\partial Y^2} = \frac{\partial I(S, Y)}{\partial Y} \int_{S_u}^S \frac{\partial^2}{\partial I^2} G(s, I(s, Y)) \frac{\partial I(s, Y)}{\partial Y} ds < 0. \quad (8)$$

Furthermore, it follows from the definition of the function

$$P_M(Y) = I(S_v, Y) \left(1 - \frac{\eta_2 I(S_v, Y)}{h_2 + I(S_v, Y)}\right) = f(I(S_v, Y))$$

that we have

$$\begin{aligned} \frac{\partial P_M(Y)}{\partial Y} &= \left(1 - \frac{\eta_2 I(S_v, Y)(I(S_v, Y) + 2h_2)}{(h_2 + I(S_v, Y))^2}\right) \frac{\partial I(S_v, Y)}{\partial Y} \\ &= \left(1 - \frac{\eta_2 I(S_v, Y)(I(S_v, Y) + 2h_2)}{(h_2 + I(S_v, Y))^2}\right) \exp\left(\int_{S_u}^{S_v} \frac{\partial}{\partial I} G(s, I(s, Y)) ds\right) \\ &= f'(I(S_v, Y)) \exp\left(\int_{S_u}^{S_v} \frac{\partial}{\partial I} G(s, I(s, Y)) ds\right) \end{aligned} \quad (9)$$

and

$$\begin{aligned}
\frac{\partial^2 P_M(Y)}{\partial Y^2} &= \frac{\partial^2 I(S_v, Y)}{\partial Y^2} + \frac{\partial^2 I(S_v, Y)}{\partial Y^2} \frac{\partial B_2(I)}{\partial I} \Big|_{I=I(S_v, Y)} \\
&\quad + \frac{\partial I(S_v, Y)}{\partial Y} \left( \frac{\partial}{\partial Y} \frac{\partial B_2(I)}{\partial I} \Big|_{I=I(S_v, Y)} \right) \\
&= (B_2'(I(S_v, Y)) + 1) \frac{\partial^2 I(S_v, Y)}{\partial Y^2} + \left( \frac{\partial I(S_v, Y)}{\partial Y} \right)^2 B_2''(I(S_v, Y)) \\
&= f'(I(S_v, Y)) \frac{\partial^2 I(S_v, Y)}{\partial Y^2} - \left( \frac{\partial I(S_v, Y)}{\partial Y} \right)^2 \frac{2\eta_2 h_2^2}{(I(S_v, Y) + h_2)^3}. \tag{10}
\end{aligned}$$

Note that if  $h_2 = 0$  then  $B_2''(0) = 0$ , thus one term  $-\frac{2\eta_2}{h_2}$  will disappear from the formula for  $\frac{\partial^2 P_M(0)}{\partial Y^2}$ . Then, it follows from the monotonicity of the function  $f(I)$  that if  $Y \in (0, I_{s_u}]$  then  $\frac{\partial P_M(Y)}{\partial Y} > 0$  and  $\frac{\partial^2 P_M(Y)}{\partial Y^2} < 0$ , which indicate that  $P_M(Y)$  is continuous and concave on the interval  $(0, I_{s_u}]$ . Further, according to the monotonicity of  $P_M(Y)$  on the interval  $(0, I_{s_u}]$  we see that  $P_M(Y)$  is monotonically decreasing on the interval  $(I_{s_u}, +\infty)$ . Therefore, it follows from  $R_0 \geq 1$  and  $S_v < K$  that  $\frac{dI}{dt} \leq 0$  for all  $S < S_v$ , which indicates that  $Y \geq \mathcal{P}(Y) > P_M(Y)$  for all  $Y \in (0, I_{s_u}] \cup (I_{s_u}, K)$  due to  $f(I) < I$ . All these results confirm that the Poincaré map  $P_M$  only has zero fixed point, i.e.  $P_M(0) = 0$ , which is globally stable. Consequently, for model (2) there exists a unique DFPS which is globally stable.

**Remark 3.** It follows from the proofs of Theorems 1 and 2 that the global stability of the DFPS can be proved by using different methods, and the methods shown in Theorem 2 could be widely employed in generalized systems.

#### 4. Bifurcation and reproduction number

Note that if  $R_0 > 1$ , then for model (1) there exists a unique endemic equilibrium  $P^*(S^*, I^*)$ . Thus, according to the positions among  $S_v$ ,  $S^*$  and  $K$  we consider the following two cases:

- (C1),  $S_v \leq S^* < K$ , i.e.  $R_0 > 1 \geq \frac{\beta S_v}{q}$ ;
- (C2),  $S^* < S_v < K$ , i.e.  $1 < \frac{\beta S_v}{q} < R_0$ .

For case (C1), any solution initiating from the line  $l_4$  will experience infinitely many impulsive effects. Moreover, it follows from  $\frac{\beta S - q}{\Lambda - \delta S} < 0$  for all  $S \in [S_u, S_v]$  due to  $S_v \leq S^*$  that we have  $J_2 + J_3 < 0$ , i.e.  $R_c < 1$ . This indicates that the DFPS is locally stable for case (C1).

Moreover, for case (C1), the Poincaré map  $P_M$  is well defined, which satisfies all properties shown in Theorem 2 by using similar methods. Thus, for case (C1) we have the following main results:

**Theorem 3.** *If  $R_0 > 1 \geq \frac{\beta S_v}{q}$  then the DFPS  $(S^T(t), 0)$  of model (2) is globally stable.*

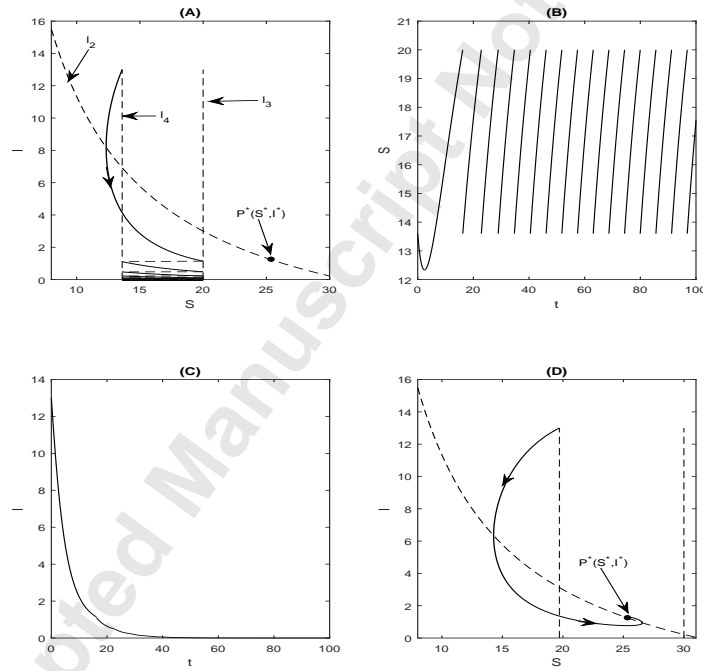


Figure 2: Illustration of the global stability of the DFPS for case (C1), i.e.  $R_0 > 1 \geq \frac{\beta S_v}{q}$ . The parameter values are as follows:  $\Lambda = 2.5$ ,  $\beta = 0.015$ ,  $\delta = 0.08$ ,  $\gamma = 0.3$ ,  $\eta_1 = 0.4$ ,  $h_1 = 5$ ,  $\eta_2 = 0.1$ ,  $h_2 = 3$  and  $S_v = 20$  in (A)-(C),  $S_v = 30$  in (D).

**Remark 4.** Under the conditions of Theorem 3, we see that the uncontrolled ODE model will be stable in the endemic state  $P^*(S^*, I^*)$ , as shown in Fig.2(D). If so, we only need to correctly choose the threshold of the susceptible population  $S_v$ , i.e.  $S_v < S^*$ , then the disease can be successfully controlled such that it quickly declines towards extinction, as shown in Fig.2(A-C).

For case (C2), since the sign of  $J_2 + J_3$  can vary, the DFPS could be unstable in this case. Thus, interesting dynamics may occur as parameter values vary. For convenience, we only need to assume that the Poincaré map  $P_M$  is well defined in the domain  $U(0^+) = [0, \epsilon)$  for  $\epsilon > 0$  small enough in the following, as shown in Fig.1(D), from which we can see that the  $P_M$  is only well defined in a small interval  $U(0^+) = [0, \epsilon)$ . Based on this assumption, we address the bifurcations related to the DFPS and discuss the threshold dynamics determined by the  $R_0$  and  $R_c$  in the following.

#### 4.1. Transcritical and pitchfork bifurcations for $\eta_1$

In this subsection we choose  $\eta_1$  as the bifurcation parameter and focus on  $h_2 \neq 0$  first. Thus, we consider  $J_2 + J_3$  as a function of  $\eta_1$ , i.e.

$$J_{12}(\eta_1) \doteq J_2 + J_3 = -\frac{\beta}{\delta}(S_v - S_u) + \frac{1}{\delta}(\beta K - q) \ln \left( \frac{K - S_u}{K - S_v} \right), \quad R_c(\eta_1) = \exp(J_{12}(\eta_1))$$

with  $S_u = S_v + B_1(S_v, \eta_1)$ . By simple calculation we have

$$\frac{\partial S_u}{\partial \eta_1} = \frac{\partial B_1(S_v, \eta_1)}{\partial \eta_1} = -\frac{S_v^2}{S_v + h_1} < 0$$

and

$$\frac{dR_c(\eta_1)}{d\eta_1} = \exp(J_{12}(\eta_1)) \frac{\partial B_1(S_v, \eta_1)}{\partial \eta_1} \left( -\frac{\beta S_u - q}{\Lambda - \delta S_u} \right).$$

Solving  $\frac{dR_c(\eta_1)}{d\eta_1} = 0$  with respect to  $\eta_1$  yields a unique root, denoted by  $\bar{\eta}_1$ , which is equivalent to the unique root of the equation  $S_u = S^*$ , i.e.

$$\bar{\eta}_1 = \left( 1 - \frac{S^*}{S_v} \right) \left( 1 + \frac{h_1}{S_v} \right) > 0.$$

In order to ensure that  $\bar{\eta}_1$  (i.e.  $0 < \bar{\eta}_1 \leq 1$ ), we need  $\frac{S_v h_1}{S_v + h_1} \leq S^* < S_v$ .



Note that if  $\eta_1 \in (0, \bar{\eta}_1)$  then we have  $S_u > S^*$  and  $\frac{dR_c(\eta_1)}{d\eta_1} > 0$ ; if  $\eta_1 \in (\bar{\eta}_1, 1)$  then we have  $S_u < S^*$  and  $\frac{dR_c(\eta_1)}{d\eta_1} < 0$ . Moreover, it follows from  $R_c(0) = 1$  and  $R_c(\bar{\eta}_1) = \exp(\int_{S^*}^{S_v} \frac{\beta s - q}{\Lambda - \delta s} ds) > 1$  that  $R_c(\eta_1) > 1$  for  $S_u > S^*$  (i.e.  $\eta_1 \in (0, \bar{\eta}_1)$ ).  
 255 Thus, the DFPS is unstable and bifurcation does not occur at all. If  $S_u < S^*$  (i.e.  $\eta_1 \in (\bar{\eta}_1, 1)$ ), then the bifurcation could occur provided that there exists an  $\eta_1^* \in (\bar{\eta}_1, 1)$  with  $R_c(\eta_1^*) = 1$ , which means that we need  $R_c(1) < 1$ . Further, according to the monotonicity of  $R_c(\eta_1)$  we conclude that  $\eta_1^*$  is unique. All these results confirm that if  $0 < \eta_1 < \eta_1^*$  then the periodic solution  $(S^T(t), 0)$   
 260 is unstable; if  $1 > \eta_1 > \eta_1^*$  then the periodic solution  $(S^T(t), 0)$  is stable. This shows that the possible bifurcation could occur at  $\eta_1 = \eta_1^*$ .

Furthermore, if  $\eta_1 = 1$  then  $S_u = \frac{h_1 S_v}{h_1 + S_v}$ . It follows from  $\frac{K - S_u}{K - S_v} > 1$  that

$$\ln \left( \frac{K - S_u}{K - S_v} \right) < \frac{\frac{K - S_u}{K - S_v} - 1}{\sqrt{\frac{K - S_u}{K - S_v}}} = \frac{S_v - S_u}{\sqrt{(K - S_u)(K - S_v)}}.$$

Therefore, we have

$$\begin{aligned} J_{12}(1) &= \frac{\beta}{\delta} \left[ -(S_v - S_u) + (K - S^*) \ln \left( \frac{K - S_u}{K - S_v} \right) \right] \\ &< \frac{\beta}{\delta} (S_v - S_u) \left[ -1 + \frac{(K - S^*)}{\sqrt{(K - S_u)(K - S_v)}} \right]. \end{aligned}$$

That is, in order to ensure that  $J_{12}(1) < 0$  (i.e.  $R_c(1) < 1$ ), we only need  $K - S^* < \sqrt{(K - S_v)(K - S_u)}$ , i.e.  $\frac{h_1 S_v}{h_1 + S_v} < K - \frac{(K - S^*)^2}{K - S_v}$  with  $K - \frac{(K - S^*)^2}{K - S_v} < S^*$ . According to

$$0 < \frac{h_1 S_v}{h_1 + S_v} < K - \frac{(K - S^*)^2}{K - S_v} = S^* \left[ R_0 - \frac{(R_0 - 1)^2}{R_0 - \frac{S_v}{S^*}} \right]$$

we have  $S^* > K - \sqrt{K(K - S_v)}$  (i.e.  $R_0 > \frac{1}{2 - \frac{S_v}{S^*}} > 1$ ). Based on the above discussion, we have the following main results related to the bifurcation parameter  $\eta_1$  and reproduction number  $R_c$ .

265 **Theorem 4.** *If  $1 < \frac{S_v}{S^*} < R_0$ ,  $R_c(1) < 1$  and  $M \doteq \frac{\partial^2 I(S_v, 0)}{\partial Y^2} < \frac{2\eta_2}{h_2}$ , then  $P_M(Y, \eta_1)$  and the transcritical bifurcation occurs at  $\eta_1 = \eta_1^*$ . That is, a stable positive fixed point of the  $P_M(Y, \eta_1)$  appears when the parameter  $\eta_1$  changes through  $\eta_1^*$  from right to left. Correspondingly, system (2) has a stable positive*

periodic solution if  $\eta_1 \in (\eta_1^* - \epsilon, \eta_1^*)$  with  $\epsilon > 0$  small enough. However, if  
 270  $M > \frac{2\eta_2}{h_2}$ , an unstable positive fixed point of the  $P_M(Y, \eta_1)$  appears when the  
 parameter  $\eta_1$  changes through  $\eta_1^*$  from left to right. Correspondingly, system (2)  
 has an unstable positive periodic solution if  $\eta_1 \in (\eta_1^*, \eta_1^* + \epsilon)$  with  $\epsilon > 0$  small  
 enough.

**Proof 3.** Since  $P_M(Y, \eta_1)$  is well defined in the domain  $U(0^+) = [0, \epsilon)$ , we  
 275 see that it is continuous and differentiable. In order to prove Theorem 4, we  
 only need to verify that  $P_M$  satisfies the four conditions of Lemma A.2 in the  
 Appendix.

Letting  $I(S; S_u, Y) = I(S, Y)$ , we have  $P_M(Y, \eta_1) = I(S_v, Y)$  and  $P_M(0, \eta_1) =$   
 $I(S_v, 0) = 0$ , which indicates that the first condition of Lemma A.2 holds true.  
 According to the inequality (9) we have

$$\frac{\partial P_M(0, \eta_1)}{\partial Y} = \exp\left(\int_{S_u}^{S_v} \frac{\beta S - q}{\Lambda - \delta S} dS\right) = R_c(\eta_1).$$

Thus,  $\frac{\partial P_M(0, \eta_1^*)}{\partial Y} = R_c(\eta_1^*) = 1$  and the second condition of Lemma A.2 follows.

By simple calculations we have

$$\begin{aligned} \frac{\partial^2 P_M(0, \eta_1)}{\partial Y \partial \eta_1} &= \frac{\partial S_u}{\partial \eta_1} \frac{\partial}{\partial S_u} \left( \frac{\partial P_M(0, \eta_1)}{\partial Y} \right) = \frac{\partial S_u}{\partial \eta_1} \frac{\partial}{\partial S_u} \left( \frac{\partial I(S_v, Y)}{\partial Y} \right) \\ &= \left( \frac{\partial I(S_v, Y)}{\partial Y} \right) \frac{\partial S_u}{\partial \eta_1} \frac{\partial}{\partial S_u} \int_{S_u}^{S_v} \frac{\partial G(s, I(s, 0))}{\partial Y} ds = \frac{dR_c(\eta_1)}{d\eta_1}, \end{aligned} \quad (11)$$

280 which indicates that  $\frac{\partial^2 P_M(0, \eta_1)}{\partial Y \partial \eta_1} = \frac{dR_c(\eta_1^*)}{d\eta_1} < 0$ , and the third condition of Lemma  
 A.2 follows.

Further, it follows from inequality (10) that

$$\frac{\partial^2 P_M(0, \eta_1)}{\partial Y^2} = \exp(J_{12}) \int_{S_u}^{S_v} \frac{\partial^2}{\partial I^2} (G(s, I(s, 0))) \frac{\partial I(s, 0)}{\partial Y} ds - \frac{2\eta_2}{h_2} \exp(2J_{12}). \quad (12)$$

Denote

$$\begin{aligned} l_1(s) &= \int_{S_u}^s \frac{\beta s - q}{\Lambda - \delta s} ds, \\ k_1(s) &= \frac{\partial I(s, 0)}{\partial Y} = \exp\left(\int_{S_u}^s \frac{\beta s - q}{\Lambda - \delta s} ds\right) = \exp l_1(s), \end{aligned}$$

and it is easy to know that  $k_1(S_u) = 1$  and  $k_1(S_v) = R_c(\eta_1)$ . Taking the derivative of  $l_1(s)$  with respect to  $s$  yields

$$l_1'(s) = \frac{\beta s - q}{\Lambda - \delta s}.$$

Letting

$$l_2(s) = \frac{\partial^2}{\partial I^2} G(s, I(s, 0)) = \frac{2\beta s(-q + \beta s)}{(\Lambda - \delta s)^2}, \quad k_2(s) = \frac{l_2(s)}{l_1'(s)} = \frac{2\beta s}{\Lambda - \delta s} = \frac{2}{h(s)},$$

and  $S_{u\eta_1^*} = (1 - \frac{\eta_1^* S_v}{S_v + h_1}) S_v$ , then we have

$$\frac{\partial^2 P_M(0, \eta_1^*)}{\partial Y^2} = \frac{\partial^2 I(S_v, 0)}{\partial Y^2} - \frac{2\eta_2}{h_2}, \quad (13)$$

where

$$\begin{aligned} M &\doteq \frac{\partial^2 I(S_v, 0)}{\partial Y^2} = \int_{S_{u\eta_1^*}}^{S_v} \frac{\partial^2}{\partial I^2} (G(s, I(s, 0))) \frac{\partial I(s, 0)}{\partial Y} ds \\ &= \int_{S_{u\eta_1^*}}^{S_v} l_2(s) k_1(s) ds \\ &= \int_{S_{u\eta_1^*}}^{S_v} \frac{l_2(s)}{l_1'(s)} l_1'(s) \exp l_1(s) ds \\ &= \int_{S_{u\eta_1^*}}^{S_v} k_2(s) d(k_1(s)). \end{aligned} \quad (14)$$

285 Note that the function  $k_1(s)$  is monotonically decreasing on the interval  $[S_u, S^*]$  and monotonically increasing on the interval  $[S^*, S_v]$ , which indicates that if  $\eta_1 = \eta_1^*$  then  $k_1(S_{u\eta_1^*}) = R_c(\eta_1^*) = 1$ . Thus,  $k_1(S^*) < k_1(s) \leq 1$  for all  $s \in [S_{u\eta_1^*}, S_v]$ . According to  $k_2'(s) = \frac{2\Lambda\beta}{(\Lambda - \beta s)^2} > 0$  for any  $s \in [S_{u\eta_1^*}, S_v]$ ,  $k_2(s)$  is a monotonically increasing function. Moreover, we have

$$\begin{aligned} \int_{S_{u\eta_1^*}}^{S_v} k_2(s) d(k_1(s)) &= k_1(s)k_2(s)|_{S_{u\eta_1^*}}^{S_v} - \int_{S_{u\eta_1^*}}^{S_v} k_1(s)k_2'(s) ds \\ &= k_2(S_v) - k_2(S_{u\eta_1^*}) - \int_{S_{u\eta_1^*}}^{S_v} k_1(s)k_2'(s) ds \\ &= \int_{S_{u\eta_1^*}}^{S_v} (1 - k_1(s))k_2'(s) ds, \end{aligned} \quad (15)$$

290 which means that  $0 < M < (1 - k_1(S^*))(k_2(S_v) - k_2(S_{u\eta_1^*}))$ .

Therefore, if  $1 \leq \frac{S_v}{S^*} < R_0$ ,  $R_c(1) < 1$  and  $M \neq \frac{2\eta_2}{h_2}$ , then the transcritical bifurcation occurs at  $\eta_1 = \eta_1^*$ . Furthermore, if  $M > \frac{2\eta_2}{h_2}$ , then  $P_M(Y, \eta_1)$  generates an unstable fixed point when  $\eta_1$  passes  $\eta_1^*$  from left to right. That is, for

$\eta_1 \in (\eta_1^*, \eta_1^* + \epsilon)$  with  $\epsilon > 0$  small enough, an unstable positive periodic solution  
 295 exists for model (2), as shown in Fig.1(D). While, if  $M < \frac{2\eta_2}{h_2}$ , then  $P_M(Y, \eta_1)$   
 exists with a positive stable fixed point when  $\eta_1$  goes through  $\eta_1^*$  from right to  
 left. That is, for  $\eta_1 \in (\eta_1^* - \epsilon, \eta_1^*)$  with  $\epsilon > 0$  small enough, a stable positive  
 periodic solution exists for model (2).

**Corollary 1.** If  $1 < \frac{\beta S_v}{q} < R_0$ ,  $R_c(1) < 1$  and  $M > \frac{2\eta_2}{h_2}$ , system (2) undergoes  
 300 the backward bifurcation at  $\eta_1 \in (\eta_1^*, \eta_1^* + \epsilon)$  with  $\epsilon > 0$  small enough.

Note that the condition  $R_c(1) < 1$  can be replaced by the inequality  $\frac{h_1 S_v}{h_1 + S_v} <$   
 $K - \frac{(K - S^*)^2}{K - S_v}$ . It follows from the conditions of Corollary 1 that the positive  
 equilibrium  $P^*$  exists which is stable for model (2) due to  $S_v > S^*$ . Moreover,  
 the DFPS  $(S^T(t), 0)$  is stable for all  $\eta_1 \in (\eta_1^*, 1)$ , i.e. we have  $R_c(\eta_1) < 1$  for all  
 305  $\eta_1 \in (\eta_1^*, 1)$ . Therefore, the stable DFPS  $(S^T(t), 0)$  and stable equilibrium  $P^*$   
 can coexist, as shown in Fig.1(D), and there exists an unstable order-1 periodic  
 solution which is bifurcated from  $(S^T(t), 0)$  once the parameter  $\eta_1$  increases and  
 exceeds the critical value  $\eta_1^*$ . Obviously, the transcritical bifurcation generates a  
 backward bifurcation, which is a novel result generated by the state-dependent  
 310 pulse vaccination model (2).

In the following, we address the special case, i.e.  $M = \frac{2\eta_2}{h_2}$ . For this special  
 case we only need to calculate  $\frac{\partial^3 P_M(0, \eta_1^*)}{\partial Y^3}$ , i.e.

$$\begin{aligned}
 \frac{\partial^3 P_M(0, \eta_1^*)}{\partial Y^3} &= \frac{\partial^3 I(S_v, 0)}{\partial Y^3} + 3 \int_{S_{u\eta_1^*}}^{S_v} k_2(s) d(\exp l_1(s)) B_2''(0) + B_2'''(0) \\
 &= \frac{\partial^3 I(S_v, 0)}{\partial Y^3} - \frac{6\eta_2}{h_2} M + \frac{6\eta_2}{h_2^2} \\
 &= \frac{\partial^3 I(S_v, 0)}{\partial Y^3} - \frac{12\eta_2^2}{h_2^2} + \frac{6\eta_2}{h_2^2},
 \end{aligned} \tag{16}$$

where

$$\frac{\partial^3 I(S_v, 0)}{\partial Y^3} = \frac{4\eta_2^2}{h_2^2} + \frac{\partial}{\partial Y} \left( \int_{S_{u\eta_1^*}}^{S_v} \frac{\partial^2}{\partial I^2} (G(s, I(s, 0))) \frac{\partial I(s, 0)}{\partial Y} ds \right) \tag{17}$$

and

$$\frac{\partial}{\partial Y} \left( \int_{S_{u\eta_1^*}}^{S_v} \frac{\partial^2}{\partial I^2} (G(s, I(s, 0))) \frac{\partial I(s, 0)}{\partial Y} ds \right) = \int_{S_{u\eta_1^*}}^{S_v} l_2(s) k_1(s) \left[ \frac{3}{2} k_1(s) k_2(s) + l_1(s) \right] ds. \tag{18}$$

315 Therefore, according to Lemma A.3 we have the following main results for this special case:

**Theorem 5.** *If  $1 < \frac{S_v}{S^*} < R_0$ ,  $R_c(1) < 1$ ,  $M = \frac{2\eta_2}{h_2}$  and  $\frac{\partial^3 P_M(0, \eta_1^*)}{\partial Y^3} \neq 0$  then the Poincaré map of system (2) occurs with a pitchfork bifurcation at  $\eta_1^*$ . Furthermore, if  $\frac{\partial^3 P_M(0, \eta_1^*)}{\partial Y^3} < 0$ , then the Poincaré map (2) occurs with a subcritical pitchfork bifurcation such that it appears as a stable positive fixed point; if*  
 320  *$\frac{\partial^3 P_M(0, \eta_1^*)}{\partial Y^3} > 0$ , then the Poincaré map (2) occurs with a supercritical pitchfork bifurcation such that it appears as an unstable positive fixed point.*

Note that the formula of  $R_c$  depends on the  $h_2$ , in particular if  $h_2 = 0$  then we have  $R_c(\eta_1) = (1 - \eta_2) \exp(J_{12}(\eta_1))$ , thus  $R_c(0) = 1 - \eta_2$ ,  $R_c(\bar{\eta}_1) > 1 - \eta_2$ . It follows from the monotonicity of  $J_{12}(\eta_1)$  that  $R_c(\eta_1)$  is monotonically increasing on the interval  $[0, \bar{\eta}_1]$  and monotonically decreasing on the interval  $(\bar{\eta}_1, 1)$ . In order to ensure that  $\eta_1^*$  exists and satisfies  $R_c(\eta_1^*) = 1$ , we need  $R_c(\bar{\eta}_1) > 1$  which indicates that  $\eta_1^* \in (0, \bar{\eta}_1)$ . Further, if we have  $R_c(1) < 1$  then there exists a unique  $\eta_1^{**} \in (\bar{\eta}_1, 1)$  such that  $R_c(\eta_1^{**}) = 1$ . Therefore, if both the  $\eta_1^*$  and  $\eta_1^{**}$  exist, then we have

$$\begin{aligned} \frac{\partial^2 P_M(0, \eta_1^*)}{\partial Y \partial \eta_1} &= \frac{dR_c(\eta_1^*)}{d\eta_1} > 0, & \frac{\partial^2 P_M(0, \eta_1^{**})}{\partial Y \partial \eta_1} &= \frac{dR_c(\eta_1^{**})}{d\eta_1} < 0, \\ \frac{\partial^2 P_M(0, \eta_1^*)}{\partial Y^2} &= M > 0, & \frac{\partial^2 P_M(0, \eta_1^{**})}{\partial Y^2} &= M > 0, \end{aligned}$$

and consequently we have the following main result:

**Corollary 2.** *If  $h_2 = 0$ ,  $1 < \frac{S_v}{S^*} < R_0$ ,  $R_c(\bar{\eta}_1) > 1$  and  $R_c(1) < 1$ , then*  
 325  *$P_M(Y, \eta_1)$  occurs with the transcritical bifurcation at  $\eta_1 = \eta_1^*$  and  $\eta_1 = \eta_1^{**}$ . That is, an unstable positive fixed point of the  $P_M(Y, \eta_1)$  appears when the parameter  $\eta_1$  changes through  $\eta_1^*$  from right to left or through  $\eta_1^{**}$  from left to right. Correspondingly, system (2) has an unstable positive periodic solution if  $\eta_1 \in (\eta_1^* - \epsilon, \eta_1^*)$  or  $\eta_1 \in (\eta_1^{**}, \eta_1^{**} + \epsilon)$  with  $\epsilon > 0$  small enough.*

Note that when  $h_2 = 0$ , we could choose  $\eta_2$  as a bifurcation parameter. If so, we have

$$R_c(\eta_2) = (1 - \eta_2) \exp(J_1 + J_2).$$

330 Letting  $R_c(\eta_2) = 1$  and solving it one has  $\eta_2^* = 1 - \exp(-J_1 - J_2)$  such that  $R_c(\eta_2^*) = 1$  which requires  $J_1 + J_2 > 0$  to ensure that  $\eta_2^*$  is well defined. Moreover,  $S_u > S^*$  implies  $J_1 + J_2 > 0$  holds true.

It follows from (4) that

$$J_2 + J_3 = \frac{q}{\delta} \left[ (R_0 - 1) \ln \left( \frac{R_0 - \frac{S_u}{S^*}}{R_0 - \frac{S_v}{S^*}} \right) - \left( \frac{S_v}{S^*} - \frac{S_u}{S^*} \right) \right].$$

Denote the function  $\omega_4(x) \doteq (R_0 - 1) \ln(R_0 - x) + x$  with  $\omega_4'(x) = \frac{1-x}{R_0-x}$ . Thus,  $\omega_4(x)$  is monotonically increasing on the interval  $[0, 1)$ , and decreasing on the interval  $[1, R_0)$ . Moreover,  $x = R_0$  is an asymptote of the function  $\omega_4(x)$ , and both  $\frac{S_u}{S^*}$  and  $\frac{S_v}{S^*} \in [0, R_0)$ , then we have

$$J_2 + J_3 = \frac{q}{\delta} \left[ \omega_4\left(\frac{S_u}{S^*}\right) - \omega_4\left(\frac{S_v}{S^*}\right) \right].$$

It follows from the monotonicity of the function  $\omega_4(x)$  that if  $S_u > S^*$  then  $J_2 + J_3 > 0$ . Moreover,  $\omega_4\left(\frac{S_v}{S^*}\right) < \omega_4(0) = (R_0 - 1) \ln(R_0)$  also indicates that  $J_2 + J_3 > 0$ . Solving the inequality  $\omega_4\left(\frac{S_v}{S^*}\right) < (R_0 - 1) \ln(R_0)$  one has  $\frac{S_v}{S^*} \geq (R_0 - 1) \text{LambertW}\left(-\frac{R_0}{R_0-1} \exp\left(-\frac{R_0}{R_0-1}\right)\right) + R_0 \doteq \zeta$ , and it is easy to see that  $\zeta \in (1, R_0)$ , where the definition and properties of the Lambert W function can be found in references [27, 29, 31]. Therefore,

$$\frac{\partial P_M(0, \eta_2)}{\partial Y} = R_c(\eta_2), \quad \frac{\partial^2 P_M(0, \eta_2)}{\partial Y \partial \eta_2} = \frac{dR_c(\eta_2)}{d\eta_2} = -\exp(J_1 + J_2) < 0$$

and

$$\frac{\partial^2 P_M(0, \eta_2^*)}{\partial Y^2} = M > 0.$$

By methods similar to those above we can evaluate the conditions of Lemma A.2, to give the following main results:

335 **Corollary 3.** *If  $h_2 = 0$ ,  $1 < \frac{\beta S_v}{q} < R_0$  and  $J_2 + J_3 > 0$ , then  $P_M(Y, \eta_2)$  occurs with the transcritical bifurcation at  $\eta_2 = \eta_2^*$ . That is, an unstable positive fixed point of the  $P_M(Y, \eta_2)$  appears when the parameter  $\eta_2$  changes through  $\eta_2^*$  from left to right. Correspondingly, system (2) has an unstable positive periodic solution if  $\eta_2 \in (\eta_2^*, \eta_2^* + \epsilon)$  with  $\epsilon > 0$  small enough. Particular-*  
 340 *ly, the condition of  $J_2 + J_3 > 0$  can be strengthened to be  $1 \leq \frac{S_u}{S^*}$  or  $\frac{S_v}{S^*} \geq (R_0 - 1) \text{LambertW}\left(-\frac{R_0}{R_0-1} \exp\left(-\frac{R_0}{R_0-1}\right)\right) + R_0$ .*

#### 4.2. Transcritical bifurcation for threshold level $S_v$

In this subsection, we choose the threshold level  $S_v$  as a bifurcation parameter, which can help us to evaluate how to determine the number in the population to be vaccinated such that the disease could be eradicated. To do this, we consider the control reproduction number  $R_c$  as a function of  $S_v$ , i.e. we have  $R_c(S_v) = \exp(J_{12}(S_v))$  and

$$\begin{aligned} J_{12}(S_v) \doteq J_2 + J_3 &= \int_{S_u}^{S_v} \frac{\beta s - q}{\Lambda - \delta s} ds \\ &= -\frac{\beta}{\delta}(S_v - S_u) + \frac{1}{\delta}(\beta K - q) \ln \left( \frac{K - S_u}{K - S_v} \right). \end{aligned}$$

By simple calculations we have

$$\frac{dR_c(S_v)}{dS_v} = \exp(J_{12}(S_v)) \frac{dJ_{12}(S_v)}{dS_v}$$

and

$$\frac{dJ_{12}(S_v)}{dS_v} = \frac{\partial}{\partial S_v} \int_{S_u}^{S_v} \frac{\beta s - q}{\Lambda - \delta s} ds,$$

where  $S_u = S_v + B_1(S_v)$ . Letting  $\omega_3(x) \doteq \frac{\beta x - q}{\Lambda - \delta x} = \frac{\beta(x - S^*)}{\delta(K - x)}$ , one has

$$\frac{dJ_{12}(S_v)}{dS_v} = \omega_3(S_v) - (1 + I_1'(S_v))\omega_3(S_u). \quad (19)$$

If  $S_u \leq S^*$ , then  $\omega_3(S_u) \leq 0$ . It follows from  $1 + I_1'(S_v) > 0$  that  $\frac{dJ_{12}(S_v)}{dS_v} > 0$ ; If  $S_u > S^*$ , then  $\omega_3(S_u) > 0$ . Taking the derivative of  $\omega_3(x)$  with respect to  $x$  yields

$$\omega_3'(x) = \frac{q}{\delta} \frac{R_0 - 1}{(K - x)^2} > 0.$$

Thus, we have

$$\begin{aligned} \omega_3(S_v) - (1 + I_1'(S_v))\omega_3(S_u) &> \omega_3(S_u) - (1 + I_1'(S_v))\omega_3(S_u) \\ &= (-I_1'(S_v))\omega_3(S_u) > 0. \end{aligned} \quad (20)$$

In conclusion, no matter what the position between  $S_u$  and  $S^*$  is, we always have  $\frac{dJ_{12}(S_v)}{dS_v} > 0$ , i.e.  $J_{12}(S_v)$  is a monotonically increasing function of  $S_v$ . Moreover, we have

$$\lim_{S_v \rightarrow S^*} J_{12}(S_v) = \lim_{S_v \rightarrow S^*} \int_{S_u}^{S_v} \omega_3(x) dx = \int_{S^* + B_1(S^*)}^{S^*} \omega_3(x) dx < 0$$

and

$$\lim_{S_v \rightarrow K} J_{12}(S_v) = \lim_{S_v \rightarrow K} \frac{q}{\delta} [(R_0 - 1) \ln \left( \frac{K - S_u}{K - S_v} \right) - \frac{\beta}{q} (S_v - S_u)] = +\infty.$$

It follows from the continuity of the function  $J_{12}(S_v)$  that there exists a unique  $S_v^* \in (S^*, K)$  such that  $J_{12}(S_v^*) = 0$ , i.e. there is a unique  $S_v^* \in (S^*, K)$  such that  $R_c(S_v^*) = 1$ . Further, by simple calculations we have

$$\frac{\partial P_M(0, S_v)}{\partial Y} = R_c(S_v)$$

and

$$\frac{\partial^2 P_M(0, S_v)}{\partial Y \partial S_v} = \frac{dR_c(S_v)}{dS_v} > 0.$$

345 By employing similar methods to those shown in Theorem 4 we can address the signs of  $\frac{\partial^2 P_M(0, S_v^*)}{\partial^2 Y}$  and  $\frac{\partial^3 P_M(0, S_v^*)}{\partial^3 Y}$ . Therefore, we have the following main results:

**Theorem 6.** *If  $1 < \frac{S_v}{S^*} < R_0$  and  $M < \frac{2\eta_2}{h_2}$ , then  $P_M(Y, S_v)$  occurs with the transcritical bifurcation at  $S_v = S_v^*$ . That is, a stable positive fixed point of*  
 350 *the  $P_M(Y, S_v)$  appears when the parameter  $S_v$  changes through  $S_v^*$  from left to right. Correspondingly, system (2) has a stable positive periodic solution if  $S_v \in (S_v^*, S_v^* + \epsilon)$  with  $\epsilon > 0$  small enough. Moreover, if  $M > \frac{2\eta_2}{h_2}$ , an unstable positive fixed point of the  $P_M(Y, S_v)$  appears when the parameter  $S_v$  changes through  $S_v^*$  from right to left. Correspondingly, system (2) has an unstable*  
 355 *positive periodic solution if  $S_v \in (S_v^* - \epsilon, S_v^*)$  with  $\epsilon > 0$  small enough.*

**Theorem 7.** *If  $1 < \frac{S_v}{S^*} < R_0$ ,  $M = \frac{2\eta_2}{h_2}$  and  $\frac{\partial^3 P_M(0, S_v^*)}{\partial Y^3} \neq 0$ , then the Poincaré map of system (2) occurs with a pitchfork bifurcation at  $S_v^*$ . Furthermore, if  $\frac{\partial^3 P_M(0, S_v^*)}{\partial Y^3} < 0$ , then the Poincaré map (2) occurs with a supercritical pitchfork bifurcation such that it appears as a stable positive fixed point; if  $\frac{\partial^3 P_M(0, S_v^*)}{\partial Y^3} > 0$ ,*  
 360 *then the Poincaré map (2) occurs with a subcritical pitchfork bifurcation such that it appears as an unstable positive fixed point.*

Similarly, for the special case  $h_2 = 0$  we have

$$R_c(S_v) = (1 - \eta_2) \exp(J_{12}(S_v))$$



and according to the properties of the function  $J_{12}(S_v)$  we have  $\frac{\partial^2 P_M(0, S_v)}{\partial Y \partial S_v} = \frac{dR_c(S_v)}{dS_v} > 0$ , which indicates that there exists a unique  $S_v^*$  such that  $J_{12}(S_v^*) = \ln(\frac{1}{1-\eta_2}) > 0$ , i.e.  $R_c(S_v^*) = 1$ . It follows from  $\frac{\partial^2 P_M(0, S_v^*)}{\partial Y^2} = M > 0$  and Lemma

365 A.2 that

**Corollary 4.** *If  $h_2 = 0$ ,  $1 < \frac{\beta S_v}{q} < R_0$ , then  $P_M(Y, S_v)$  occurs with the trans-critical bifurcation at  $S_v = S_v^*$ , i.e. an unstable positive fixed point of the  $P_M(Y, S_v)$  appears when the parameter  $S_v$  changes through  $S_v^*$  from right to left. Correspondingly, system (2) has an unstable positive periodic solution if*

370  $S_v \in (S_v^* - \epsilon, S_v^*)$  with  $\epsilon > 0$  small enough.

#### 4.3. Trans-critical bifurcation for $\Lambda$

In this subsection we choose  $\Lambda$  as a bifurcation parameter, i.e. we denote  $R_c(\Lambda) = \exp(J_{12}(\Lambda)) = P_M(0, \Lambda)$  and

$$\begin{aligned} J_{12}(\Lambda) \doteq J_2 + J_3 &= \int_{S_u}^{S_v} \frac{\beta s - q}{\Lambda - \delta s} ds \\ &= -\frac{\beta}{\delta} (S_v - S_u) + \frac{1}{\delta} (-q + \beta(\frac{\Lambda}{\delta})) \ln(\frac{-\delta S_u + \Lambda}{-\delta S_v + \Lambda}). \end{aligned}$$

with

$$\lim_{\frac{\Lambda}{\delta} \rightarrow +\infty} J_{12}(\Lambda) = 0, \quad \lim_{\frac{\Lambda}{\delta} \rightarrow S_v} J_{12}(\Lambda) = +\infty.$$

By calculations we have

$$\begin{aligned} \frac{dR_c(\Lambda)}{d\Lambda} &= \frac{\partial P_M(0, \Lambda)}{\partial Y} = R_c(\Lambda) \frac{dJ_{12}(\Lambda)}{d\Lambda}, \\ \frac{dJ_{12}(\Lambda)}{d\Lambda} &= -\int_{S_u}^{S_v} \frac{\beta s - q}{(\Lambda - \delta s)^2} ds \\ &= -(S_v - S_u) \frac{\frac{\beta \Lambda}{\delta} - q}{(\Lambda - \delta S_v)(\Lambda - \delta S_u)} + \frac{\beta}{\delta^2} \ln(\frac{-\delta S_u + \Lambda}{-\delta S_v + \Lambda}) \end{aligned}$$

and  $\lim_{\Lambda \rightarrow +\infty} \frac{dJ_{12}(\Lambda)}{d\Lambda} = 0$ . Moreover, we have

$$\begin{aligned} \frac{dJ_{12}^2(\Lambda)}{d\Lambda^2} &= \int_{S_u}^{S_v} \frac{2(\beta s - q)}{(\Lambda - \delta s)^3} ds \\ &= -\frac{\beta(S_u - S_v)[(S_u + S_v - 2S^*)\Lambda - (2S_u S_v - S^*(S_u + S_v))\delta]}{(-S_v \delta + \Lambda)^2 (-S_u \delta + \Lambda)^2}. \end{aligned}$$

If  $S^* = \frac{S_v + S_u}{2}$ , then we have  $\frac{2}{\frac{1}{S_v} + \frac{1}{S_u}} < S^*$  and

$$\frac{dJ_{12}^2(\Lambda)}{d\Lambda^2} = \int_{S_u}^{S_v} \frac{2(\beta s - q)}{(\Lambda - \delta s)^3} ds = \frac{\beta(S_v - S_u)[-(\frac{2}{\frac{1}{S_v} + \frac{1}{S_u}} - S^*)(S_u + S_v)\delta]}{(-S_v \delta + \Lambda)^2 (-S_u \delta + \Lambda)^2} > 0,$$

which indicates that  $\frac{dJ_{12}(\Lambda)}{d\Lambda}$  is monotonically increasing on the interval  $(S_v\delta, +\infty)$ .

Moreover, it follows from  $\lim_{\Lambda \rightarrow +\infty} \frac{dJ_{12}(\Lambda)}{d\Lambda} = 0$  that  $\frac{dJ_{12}(\Lambda)}{d\Lambda} < 0$  for all  $\Lambda \in (S_v\delta, +\infty)$ , i.e.  $J_{12}(\Lambda)$  is monotonically decreasing on the interval  $(S_v\delta, +\infty)$ .

375 All these results confirm that  $J_{12}(\Lambda) > 0$  (i.e.  $R_c(\Lambda) > 1$ ) for all  $\Lambda \in (\delta S_v, +\infty)$ ,

which means that the DFPS is unstable and no bifurcation occurs with respect to  $\Lambda$ . If  $S^* \neq \frac{S_v+S_u}{2}$ , then solving  $\frac{dJ_{12}^2(\Lambda)}{d\Lambda^2} = 0$  yields  $\tilde{\Lambda} = \delta \left( \frac{\frac{2S_v S_u}{S_v+S_u} - S^*}{(\frac{S_u+S_v}{2} - S^*) \frac{2}{S_v+S_u}} \right)$ .

For the bifurcation related to the parameter  $\Lambda$ , we consider the following cases:

(i) If  $\frac{S_v+S_u}{2} > \frac{2}{\frac{1}{S_v} + \frac{1}{S_u}} > S^*$  then we have  $\tilde{\Lambda} > 0$ .

380 (a) For this case we first consider  $\tilde{\Lambda} > \delta S_v$ , and we have  $\frac{dJ_{12}^2(\Lambda)}{d\Lambda^2} < 0$

for  $\Lambda \in (\delta S_v, \tilde{\Lambda}]$ ;  $\frac{dJ_{12}^2(\Lambda)}{d\Lambda^2} \geq 0$  for all  $\Lambda \in [\tilde{\Lambda}, +\infty)$ . Correspondingly, the function  $\frac{dJ_{12}(\Lambda)}{d\Lambda}$  is monotonically decreasing on the interval

$(\delta S_v, \tilde{\Lambda}]$  and monotonically increasing on the interval  $[\tilde{\Lambda}, +\infty)$ .

Moreover,  $\lim_{\Lambda \rightarrow +\infty} \frac{dJ_{12}(\Lambda)}{d\Lambda} = 0$ , thus we have  $\frac{dJ_{12}(\Lambda)}{d\Lambda} < 0$  for all

385  $\Lambda \in [\tilde{\Lambda}, +\infty)$ . Now we claim that  $\frac{dJ_{12}(\Lambda)}{d\Lambda} < 0$  for all  $\Lambda \in (\delta S_v, \tilde{\Lambda}]$ .

Otherwise, we assume that there exists a unique  $\hat{\Lambda} \in (\delta S_v, \tilde{\Lambda})$  such that  $\frac{dJ_{12}(\hat{\Lambda})}{d\Lambda} = 0$ , then we have  $\frac{dJ_{12}(\Lambda)}{d\Lambda} \geq 0$  for all  $\Lambda \in (\delta S_v, \hat{\Lambda}]$  and  $\frac{dJ_{12}(\Lambda)}{d\Lambda} < 0$

for all  $\Lambda \in (\hat{\Lambda}, +\infty)$ . Consequently,  $J_{12}(\Lambda)$  is monotonically increasing

on the interval  $(\delta S_v, \hat{\Lambda}]$  and decreasing on the interval  $(\hat{\Lambda}, +\infty)$ ,

390 which contradicts  $\lim_{\frac{\Lambda}{\delta} \rightarrow +\infty} J_{12}(\Lambda) = 0$  and  $\lim_{\frac{\Lambda}{\delta} \rightarrow S_v} J_{12}(\Lambda) = +\infty$ .

Therefore,  $\frac{dJ_{12}(\Lambda)}{d\Lambda} < 0$  for all  $\Lambda \in (\delta S_v, +\infty)$  and  $J_{12}(\Lambda)$  is monotonically decreasing on  $(S_v\delta, +\infty)$ , with  $J_{12}(\Lambda) > 0$  for all  $\Lambda \in (\delta S_v, +\infty)$ .

All these results confirm that the DFPS is unstable and the bifurcation does not occur at all for this case.

395 (b) When  $\tilde{\Lambda} \leq \delta S_v$ , from which we have  $\frac{dJ_{12}^2(\Lambda)}{d\Lambda^2} > 0$  for all  $\Lambda \in (\delta S_v, +\infty)$ .

Thus,  $\frac{dJ_{12}(\Lambda)}{d\Lambda}$  is monotonically increasing on the interval  $(\delta S_v, +\infty)$

with  $\lim_{\Lambda \rightarrow +\infty} \frac{dJ_{12}(\Lambda)}{d\Lambda} = 0$ , which means that  $\frac{dJ_{12}(\Lambda)}{d\Lambda} < 0$  for all

$\Lambda \in (S_v\delta, +\infty)$  and  $J_{12}(\Lambda)$  is monotonically decreasing on  $(S_v\delta, +\infty)$ .

According to  $\lim_{\frac{\Lambda}{\delta} \rightarrow +\infty} J_{12}(\Lambda) = 0$  we have  $J_{12}(\Lambda) > 0$  for all  $\Lambda \in$

400  $(\delta S_v, +\infty)$  and then  $R_c(\Lambda) > 1$  holds true, and again the DFPS is

unstable and the bifurcation does not occur at all for this case.

(ii) If  $\frac{S_v+S_u}{2} > S^* \geq \frac{2}{\frac{1}{S_v}+\frac{1}{S_u}}$  then  $\tilde{\Lambda} < 0$ . For this case we have  $\frac{dJ_{12}^2(\Lambda)}{d\Lambda^2} > 0$  for all  $\Lambda \in (\delta S_v, +\infty)$ . By using methods similar to those in (b) we can show that  $J_{12}(\Lambda) > 0$  for all  $\Lambda \in (\delta S_v, +\infty)$  and  $R_c(\Lambda) > 1$ , which indicates that no bifurcation occurs at all in such case.

(iii) If  $S^* > \frac{S_v+S_u}{2} > \frac{2}{\frac{1}{S_v}+\frac{1}{S_u}}$  then  $\tilde{\Lambda} > 0$ . Now we claim that  $\tilde{\Lambda} > \delta S_v$ . Otherwise, we assume that  $\tilde{\Lambda} \leq \delta S_v$ , then we have  $\frac{dJ_{12}^2(\Lambda)}{d\Lambda^2} < 0$  for all  $\Lambda \in (\delta S_v, +\infty)$  and  $\frac{dJ_{12}(\Lambda)}{d\Lambda}$  is monotonically decreasing on  $(\delta S_v, +\infty)$ . Moreover, we have  $\lim_{\frac{\Delta}{\delta} \rightarrow +\infty} J_{12}(\Lambda) = 0$ , thus  $\frac{dJ_{12}(\Lambda)}{d\Lambda} > 0$  for all  $\Lambda \in (\delta S_v, +\infty)$ , i.e.  $J_{12}(\Lambda)$  is monotonically increasing on  $(S_v\delta, +\infty)$ , which contradicts  $\lim_{\frac{\Delta}{\delta} \rightarrow +\infty} J_{12}(\Lambda) = 0$  and  $\lim_{\frac{\Delta}{\delta} \rightarrow S_v} J_{12}(\Lambda) = +\infty$ . Thus,  $\frac{dJ_{12}^2(\Lambda)}{d\Lambda^2} \geq 0$  for all  $\Lambda \in (\delta S_v, \tilde{\Lambda}]$ , and  $\frac{dJ_{12}^2(\Lambda)}{d\Lambda^2} < 0$  for all  $\Lambda \in (\tilde{\Lambda}, +\infty)$ . Moreover, according to  $\lim_{\Lambda \rightarrow +\infty} \frac{dJ_{12}(\Lambda)}{d\Lambda} = 0$  we have  $\frac{dJ_{12}(\Lambda)}{d\Lambda} > 0$  for all  $\Lambda \in [\tilde{\Lambda}, +\infty)$ . It is easy to know that there exists a unique  $\hat{\Lambda} \in (\delta S_v, \tilde{\Lambda})$  such that  $\frac{dJ_{12}(\hat{\Lambda})}{d\Lambda} = 0$ , and  $\frac{dJ_{12}(\Lambda)}{d\Lambda} \leq 0$  for all  $\Lambda \in (\delta S_v, \hat{\Lambda}]$ ;  $\frac{dJ_{12}(\Lambda)}{d\Lambda} > 0$  for all  $\Lambda \in (\hat{\Lambda}, +\infty)$ . According to  $\lim_{\frac{\Delta}{\delta} \rightarrow +\infty} J_{12}(\Lambda) = 0$  and  $\lim_{\frac{\Delta}{\delta} \rightarrow S_v} J_{12}(\Lambda) = +\infty$  we know that there exists a unique  $\Lambda^* \in (\delta S_v, \hat{\Lambda})$  such that  $J_{12}(\Lambda^*) = 0$ , i.e.  $R_c(\Lambda^*) = 1$  with  $\frac{dJ_{12}(\Lambda^*)}{d\Lambda} < 0$  and  $\frac{dR_c(\Lambda^*)}{d\Lambda} < 0$ . By employing methods similar to those above, we can show that  $P_M(Y, \Lambda)$  will occur with the bifurcation as  $\Lambda = \Lambda^*$  for this case, which depends on the magnitude of  $M$ , i.e. if  $M \neq \frac{2\eta_2}{h_2}$  then a transcritical bifurcation occurs; if  $M = \frac{2\eta_2}{h_2}$  and  $\frac{\partial^3 P_M(0, \Lambda^*)}{\partial Y^3} \neq 0$  then a pitchfork bifurcation occurs.

In summary, if  $\frac{S_v+S_u}{2} \geq S^*$  then  $J_{12}(\Lambda)$  is monotonically decreasing on the interval  $(S_v\delta, +\infty)$ ; if  $\frac{S_v+S_u}{2} < S^*$  then  $J_{12}(\Lambda)$  is monotonically decreasing on the interval  $(\delta S_v, \hat{\Lambda}]$  and increasing on the interval  $(\hat{\Lambda}, +\infty)$ . Moreover, we have the following main results:

**Theorem 8.** Assume that  $h_2 \neq 0$ ,  $1 < \frac{S_v}{S^*} < R_0$ . If  $\frac{S_v+S_u}{2} \geq S^*$  then  $J_{12}(\Lambda)$  is monotonically decreasing on the interval  $(S_v\delta, +\infty)$  and  $R_c(\Lambda) > 1$  for all  $\Lambda$ , which means that the DFPS  $(S^T(t), 0)$  is unstable. If  $\frac{S_v+S_u}{2} < S^*$  then  $J_{12}(\Lambda)$  is monotonically decreasing on the interval  $(\delta S_v, \hat{\Lambda}]$  and increasing on the interval  $(\hat{\Lambda}, +\infty)$ . There exists a unique  $\Lambda^* \in (S_v\delta, +\infty)$  such that  $R_c(\Lambda^*) = 1$  and

$P_M(Y, \Lambda)$  occurs with a bifurcation at  $\Lambda = \Lambda^*$ . Moreover, if  $M \neq \frac{2\eta_2}{h_2}$  then a transcritical bifurcation occurs; if  $M = \frac{2\eta_2}{h_2}$  and  $\frac{\partial^3 P_M(0, \Lambda^*)}{\partial Y^3} \neq 0$ , then a pitchfork bifurcation occurs.

435 In particular, if  $h_2 = 0$ , we have  $R_c(\Lambda) = (1 - \eta_2) \exp(J_{12}(\Lambda))$  with  $\lim_{K \rightarrow +\infty} J_{12}(\Lambda) = 0$  and  $\lim_{K \rightarrow S_v} J_{12}(\Lambda) = +\infty$ , which indicate that there exists a unique  $\Lambda^* \in (S_v \delta, +\infty)$  such that  $J_{12}(\Lambda^*) = \ln \frac{1}{1 - \eta_2} > 0$ , i.e.  $R_c(\Lambda^*) = 1$  with  $\frac{dJ_{12}(\Lambda^*)}{d\Lambda} < 0$ . Based on the monotonicity of  $J_{12}(\Lambda)$  we conclude that no matter what the relationship between  $\frac{S_v + S_u}{2}$  and  $S^*$ , critical value  $\Lambda^*$  exists and is unique. Moreover, according to  $\frac{\partial^2 P_M(0, \Lambda^*)}{\partial Y^2} = M > 0$  we have the following main results:

**Corollary 5.** *If  $h_2 = 0$ ,  $1 < \frac{S_u}{S^*} < R_0$ , then  $P_M(Y, \Lambda)$  occurs with the transcritical bifurcation at  $\Lambda = \Lambda^*$ , which indicates that an unstable positive fixed point of the  $P_M(Y, \Lambda)$  appears when the parameter  $\Lambda$  changes through  $\Lambda^*$  from left to right. Correspondingly, system (2) has an unstable positive periodic solution if*

445  $\Lambda \in (\Lambda^*, \Lambda^* + \epsilon)$  with  $\epsilon > 0$  small enough.

Note that if  $h_2 = 0$  and  $P_M(Y)$  occurs with bifurcations with respect to parameters  $\eta_1, \eta_2, S_v, \Lambda$ , then we must have  $\frac{\partial^2 P_M(0, \eta_1^*)}{\partial Y^2} = \frac{\partial^2 P_M(0, \eta_2^*)}{\partial Y^2} = \frac{\partial^2 P_M(0, S_v^*)}{\partial Y^2} = \frac{\partial^2 P_M(0, \Lambda^*)}{\partial Y^2} = M > 0$ . Thus, we conclude that:

**Theorem 9.** *If  $h_2 = 0$  and  $P_M(Y)$  occurs with a bifurcation with respect to the parameters  $\eta_1, \eta_2, S_v, \Lambda$ , then it must be a transcritical bifurcation and generates an unstable interior periodic solution, i.e. a backward bifurcation occurs and bistability appears when the DFPS of model (2) and the interior equilibrium  $P^*(S^*, I^*)$  can coexist.*

## 5. Discussion

455 The basic or control reproduction number plays a key role in analyzing dynamics of epidemic models, but how to define and calculate it is challenging due to the complexity of the various control measures involved in the models. In particular, most control measures are implemented instantaneously, which

can be modelled by impulsive differential equations with fixed or unfixed mo-  
460 ments. Infectious disease models with pulse vaccination or treatment strategies  
have been widely studied recently [5, 19, 8, 10, 15, 20, 13, 7], and most of the  
models assume that the pulse vaccination or treatment tactics occur at a fixed  
period (i.e. fixed moment) resulting in non-autonomous periodic systems. If  
so, we cannot employ the theories of dynamic systems, especially the theories  
465 of impulsive dynamical systems, to study the dynamic behaviour of the model,  
and then to determine the threshold dynamic behaviour and bifurcation phe-  
nomenon of the proposed model. Therefore, in order to overcome the above  
shortcomings, in the present paper we have extended the classic SIR model of  
infections by involving state-dependent feedback control guided by a threshold  
470 size of the susceptible population, aiming to address the threshold dynamics  
and determine the threshold condition through the bifurcation theories of the  
discrete one-parameter family of maps.

The existence and global stability of the DFPS, which corresponds to the  
disease free equilibrium of the model without control actions, have been inves-  
475 tigated in detail, and the main results show that  $R_0 \leq 1$  indicates  $R_c < 1$ ,  
which reveals that the non-existence of the interior equilibrium for the classical  
SIR model (1) implies the existence and global stability of the DFPS  $(S^T(t), 0)$ .  
Moreover, if  $R_0 > 1$ , we conclude that the disease can still be completely erad-  
icated provided that a proper choice of the threshold susceptible population  
480 size  $S_v$  is made, i.e. if we choose the threshold level  $S_v < S^*$  then the DFPS  
 $(S^T(t), 0)$  could be globally stable even if  $R_0 > 1$  for the SIR model (1). All  
these results confirm that state-dependent feedback control can be effectively  
used for mitigating and eradicating infectious diseases [8, 12, 11, 13, 14, 7].

The control reproduction number  $R_c$  for model (2) could be defined based  
485 on the threshold condition for the stability of the DFPS  $(S^T(t), 0)$ . Further,  
the bifurcation analyses of the discrete one-parameter family of maps, which is  
determined by the Poincaré map of the proposed model (2), related to all in-  
teresting parameters of model (2) confirm that  $R_c$  can determine the threshold  
dynamics of model (2). In particular, the super-critical or sub-critical trans-

490 critical and pitchfork bifurcations related to the maximal vaccination rate  $\eta_1$ ,  
treatment or isolation rate  $\eta_2$ , threshold size  $S_v$  and model parameter  $\Lambda$  have  
been shown when we assume that the Poincaré map  $P_M$  is well defined in the  
neighborhood of  $U(0^+)$ .

In fact, the Poincaré map  $P_M(Y)$  is well defined for all small  $Y$  shown in  
495 Fig.2(D). Moreover, it can be confirmed from the properties of the phase portrait  
of model (1). It follows from  $S_v > S^*$  that there exists a unique trajectory  $\Gamma_2$  of  
model (1) which tangents to the line  $S = S_v$  (i.e.  $l_3$ ) at the point  $A = (S_v, I_A)$ ,  
and intersects with the line  $l_4(S = S_u)$  at the point  $C(S_u, I_c)$  with  $I_A = \frac{-\delta S_v + \Lambda}{\beta S_v}$ .  
Therefore,  $P_M(Y)$  is well defined on the domain  $[0, I_c]$  with range  $[0, f(I_A)]$ .  
500 However, since the sign of  $\frac{\partial^2 P_M(Y)}{\partial Y^2}$  on the interval  $[0, I_c]$  varies as parameters  
change, we cannot determine the convexity and concavity of  $P_M(Y)$ , which  
presents a major challenge when addressing the existence and stability of the  
order-1 periodic solution by using the properties of the Poincaré map  $P_M(Y)$ .

The existence of threshold parameter values of  $\eta_1^*, \eta_2^*, S_v^*, \Lambda^*$  for transcritical  
505 bifurcations and backward bifurcations are shown in Fig.3, which further con-  
firm that the four interesting parameters chosen for bifurcation analyses can be  
well defined. Meanwhile, the unstable interior order-1 periodic solution could  
bifurcate from the DFPS through the transcritical bifurcation, i.e. the back-  
ward bifurcation occurs, and consequently the stable DFPS of model (2) and  
510 equilibrium  $P^*$  of model (1) could coexist. Note that it follows from the main  
Theorems in Section 4 that the necessary conditions for the occurrences of the  
backward bifurcations are  $R_c < 1 < R_0$  and  $S_v > S^*$ , which show that the  
disease will have outbreaks when the control measures are not involved (i.e.  
the global stability of  $P^*$  of model (1)). Once the control measures are in-  
515 volved in the model, we conclude that the disease can be controlled even if the  
threshold level is relatively large ( $S_v > S^*$  here). Furthermore, the necessary  
condition  $R_c < 1 < R_0$  for the occurrence of a backward bifurcation implies that  
there must exist a threshold value  $\bar{R}_c$  such that the DFPS is globally stable for  
 $R_c < \bar{R}_c$ , and the stable DFPS of model (2) and equilibrium  $P^*$  of model (1)  
520 could coexist  $\bar{R}_c < R_c < 1 < R_0$ . An interesting question is how to analytically

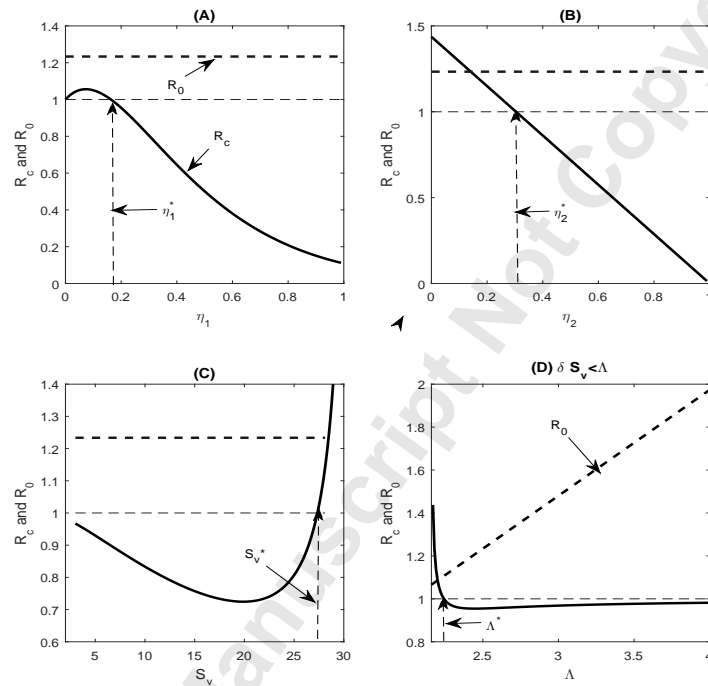


Figure 3: The existence of threshold parameter values for transcritical bifurcations for  $\eta_1^*, \eta_2^*, S_v^*, \Lambda^*$ . The base line parameter values are as follows:  $\Lambda = 2.5$ ,  $\beta = 0.015$ ,  $\delta = 0.08$ ,  $\gamma = 0.3$ ,  $h_1 = 5$ ,  $\eta_1 = 0.2$ ,  $\eta_2 = 0.1$ ,  $h_2 = 3$  and  $S_v = 27$  in (A), (D) and 29 in (B) with  $h_2 = 0$ .

determine the threshold value  $\bar{R}_c$ , a challenge for future work.

Moreover, the relations between  $R_c$  and  $R_0$  for the four interesting parameters shown in Fig.1(A) and (C) and Fig.3 reveal that no matter whether the  $R_0$  is greater than or less than 1, there is a certain parameter space that makes  $R_c$  greater than  $R_0$ . The results shown in Fig.1(A) confirm that the implementation of integrated control measures is not conducive to the elimination of disease when the control threshold level  $S_v$  is less than the critical value  $\bar{S}_v$ , and the results shown in Fig.1(C) show the importance of selecting the threshold level  $S_v$  for infectious disease control. Moreover, the results presented in Fig.3 provide an important way of thinking about how to control infectious diseases. For example, if  $-\frac{\beta}{\delta}(S_v - S^*) + \frac{1}{\delta}(\beta K - q) \ln\left(\frac{K - S^*}{K - S_v}\right) > \ln R_0$ , i.e.  $R_c(\bar{\eta}_1) > R_0$ , then  $R_c(\eta_1) > R_0$  for  $\eta_1 \in U(\bar{\eta}_1, \delta)$  (i.e. the  $\delta$  domain of  $\bar{\eta}_1$ ). Numerical simulations reveal that this phenomenon occurs only when the maximal vaccination  $\eta_1$  is very small, as shown in Fig.3(A). Note that the biphasic vaccination rate results in an inverted U-shape curve for  $\eta_1$  shown in Fig.3(A), i.e. too low a vaccination rate increases the  $R_c$  and a relatively high vaccination rate decreases the  $R_c$ . All these results confirm that increasing vaccination coverage is very important in controlling infectious diseases, especially when the implementation of the vaccination strategy depends on the size of the susceptible population.

Similarly, the biphasic threshold level  $S_v$  results in a U-shape curve shown in Fig.3(C), i.e. too small or too large a threshold level  $S_v$  is not beneficial for disease control. Moreover,  $R_c$  could be larger than  $R_0$  provided that the  $S_v$  is large enough, which can be confirmed as follows: it follows from  $\lim_{S_v \rightarrow S^*} J_{12}(S_v) < 0$ ,  $\lim_{S_v \rightarrow K} J_{12}(S_v) = +\infty$  and the continuity of  $J_{12}(S_v)$  that there exists a  $S_{v0} \in (S^*, K)$  such that  $J_{12}(S_{v0}) = \ln R_0 > 0$  (i.e.  $R_c(S_{v0}) = R_0$ ), and  $R_c(S_{v0}) > R_0$  for all  $S_v \in (S_{v0}, K)$ . Moreover, the line  $S_v = K$  is an asymptote of  $R_c(S_v)$ . Thus, we conclude that the U-shape curve related to the  $S_v$  reveals the importance of the correct selection of the threshold level to ensure the best integrated disease control effect. Note that biphasic dose response curves have been reported in many areas recently, including cancer treatment and pest control [39, 40, 41], but this is the first time that we have found that biphasic



vaccination and threshold size responses occur in an infectious disease model with state-dependent feedback control. In order to eradicate infectious diseases, the size of the susceptible population (i.e. the critical level  $S_v$  here) plays a key role, which provides important ideas and guidance for designing vaccine output and coverage according to population size and vaccine effectiveness.

The results shown in Fig.3(B) clarify that only high rates of effective treatment or isolation could successfully mitigate or eradicate the infectious disease. The birth rate  $\Lambda$  could also influence the  $R_c$  significantly, as shown in Fig.3(D). For the parameter values given in Fig.3(D) we have  $\frac{S_v+S_u}{2} = 24.72 < S^*$ , where  $S^* = 25.33$ ,  $S_u = 22.44$  and the results correspond to Theorem 8. In particular, if  $\eta_1 \leq \frac{2(S_v+h_1)(1-\frac{S^*}{S_v})}{S_v} \doteq 0.147$ , then  $R_c(\Lambda)$  is monotonically decreasing on the interval  $[\delta S_v, \infty)$  and tends to 1; If  $\eta_1 > \frac{2(S_v+h_1)(1-\frac{S^*}{S_v})}{S_v} \doteq 0.147$ , then  $R_c(\Lambda)$  is monotonically decreasing first and then increasing on the interval  $[\delta S_v, \infty)$  which will tend to 1 eventually, and this is the case shown in Fig.3(D). The relations between  $\eta_1$  and  $\frac{2(S_v+h_1)(1-\frac{S^*}{S_v})}{S_v}$  clearly reveal that how to design the vaccination campaign (i.e. choosing the vaccination rate  $\eta_1$ ) should be based on the threshold size  $S_v$  and stable population level  $S^*$  without control measures. Also, the results shown in Fig.3(D) demonstrate that for a relatively large birth rate  $\Lambda$  we must choose a high vaccination rate  $\eta_1$  such that  $R_c < 1$ . In conclusion, in order to effectively control the outbreak of infectious diseases, we should take effective, timely, measures that are stronger than usual, including vaccination, treatment and isolation, which should be adopted in relation to monitored population births and growth.

The properties of the function  $f(I) = 1 - \frac{\eta_1 I(t)}{I(t)+h_2}$  can significantly affect the monotonicity and concavity of the Poincaré map  $P_M$ , which will result in the complexity of the  $P_M$ , and consequently various different methods have been developed in the present paper to show the global stability of DFPS by considering nonlinear impulsive perturbations have in comparison with the results obtained in [38]. Moreover, it is interesting to note that the control reproduction number  $R_c = (1 - \eta_2) \exp(J_2 + J_3)$  for  $h_2 = 0$ , which indicates that the nonlinear pulse perturbation can significantly affect  $R_c$  and consequently influences the

bifurcation of  $P_M(Y)$ . In particular,  $P_M(Y)$  could only occur with a transcritical bifurcation when  $h_2 = 0$ , and the pitchfork bifurcation could occur when  
585  $h_2 > 0$ . Further, the Poincaré map  $P_M(Y, \eta_1)$  can occur with a transcritical bifurcation at  $\eta_1 = \eta_1^*$  when  $h_2 > 0$ , i.e. there exists a unique bifurcation value  $\eta_1^*$  when the nonlinear pulse is considered, while there may exist two bifurcation values once  $h_2 = 0$ .

Therefore, we conclude that the nonlinear impulsive perturbations addressed  
590 in the present paper are not only more practical and can produce rich dynamic behaviour, but also required new analytical techniques and methods to investigate their global dynamic behaviour. The idealized hypothesis proposed allowed us to simplify our model and thus conduct a thorough theoretical analysis, but undeniably it led to limitations to the application of our model to real events.  
595 Thus, we leave the interesting question of how to apply our new methods and techniques to a more general model for our future research.

## Appendix A:

The following lemma shows the local stability of the  $T$ -periodic solution of the plane impulsive semi-dynamical system.

600 **Lemma A.1.** *The  $T$ -periodic solution  $(x, y) = (\xi(t), \eta(t))$  of the system*

$$\left\{ \begin{array}{l} \frac{dx(t)}{dt} = P(x, y), \\ \frac{dy(t)}{dt} = Q(x, y), \\ \Delta x = \sigma_1(x, y), \\ \Delta y = \sigma_2(x, y), \end{array} \right\} \begin{array}{l} \text{if } \phi(x, y) \neq 0, \\ \\ \text{if } \phi(x, y) = 0, \end{array} \quad (21)$$

is orbitally asymptotically stable if the Floquet multiplier  $\mu_2$  satisfies the condition  $|\mu_2| < 1$ , where

$$\mu_2 = \prod_{k=1}^q \Delta_k \exp \left[ \int_0^T \left( \frac{\partial P}{\partial x}(\xi(t), \eta(t)) + \frac{\partial Q}{\partial y}(\xi(t), \eta(t)) \right) dt \right] \quad (22)$$

with

$$\Delta_k = \frac{P_+ \left( \frac{\partial \sigma_2}{\partial y} \frac{\partial \phi}{\partial x} - \frac{\partial \sigma_2}{\partial x} \frac{\partial \phi}{\partial y} + \frac{\partial \phi}{\partial x} \right) + Q_+ \left( \frac{\partial \sigma_1}{\partial x} \frac{\partial \phi}{\partial y} - \frac{\partial \sigma_1}{\partial y} \frac{\partial \phi}{\partial x} + \frac{\partial \phi}{\partial y} \right)}{P \frac{\partial \phi}{\partial x} + Q \frac{\partial \phi}{\partial y}},$$

and  $P$ ,  $Q$ ,  $\frac{\partial \sigma_1}{\partial x}$ ,  $\frac{\partial \sigma_1}{\partial y}$ ,  $\frac{\partial \sigma_2}{\partial x}$ ,  $\frac{\partial \sigma_2}{\partial y}$ ,  $\frac{\partial \phi}{\partial x}$  and  $\frac{\partial \phi}{\partial y}$  are calculated at the point  
605  $(\xi(t), \eta(t))$ .  $P_+ = P(\xi(t_k^+), \eta(t_k^+))$  and  $Q_+ = Q(\xi(t_k^+), \eta(t_k^+))$ . Here  $\phi(x, y)$  is a sufficiently smooth function such that  $\text{grad}\phi(x, y) \neq 0$ , and  $t_k (k \in \mathbb{N})$  is the time of the  $k$ -th jump.

The following two lemmas show the transcritical and pitchfork bifurcations of the discrete one-parameter family of maps, which can be used to address the  
610 stability and bifurcation of the Poincaré map determined by the impulsive point series of the impulsive semi-dynamical system.

**Lemma A.2.** *(Transcritical bifurcation) Let  $G : U \times I \rightarrow \mathbb{R}$  define a one-parameter family of maps, where  $G$  is  $C^r$  with  $r \geq 2$ , and  $U, I$  are open intervals of the real line containing 0. Assume that*

615 (1)  $G(0, \alpha) = 0$  for all  $\alpha$ ; (2)  $\frac{\partial G}{\partial x}(0, 0) = 1$ ;

(3)  $\frac{\partial^2 G}{\partial x \partial \alpha}(0, 0) > 0$ ; (4)  $\frac{\partial^2 G}{\partial^2 x}(0, 0) > 0$ .

Then there are  $\alpha_1 < 0 < \alpha_2$  and  $\varepsilon > 0$  such that

(i) If  $\alpha_1 < \alpha < 0$ , then  $G_\alpha = G(\cdot, \alpha)$  has two fixed points, 0 and  $x_{1\alpha} > 0$  in  $(-\varepsilon, \varepsilon)$ , then the origin is asymptotically stable and the other fixed point is

620 unstable.

(ii) If  $0 < \alpha < \alpha_2$ , then  $G_\alpha$  has two fixed points, 0 and  $x_{1\alpha} < 0$  in  $(-\varepsilon, \varepsilon)$ .

The origin is unstable, the other fixed point is asymptotically stable.

Note that the case  $\frac{\partial^2 G}{\partial x \partial \alpha}(0, 0) < 0$  is handled by making the change of parameter  $\alpha \rightarrow -\alpha$ . If the inequality (4) is reversed (i.e.  $\frac{\partial^2 G}{\partial^2 x}(0, 0) < 0$ ), then

625 (i) If  $\alpha_1 < \alpha < 0$ , then  $G_\alpha$  has two fixed points, 0 and  $x_{1\alpha} < 0$  in  $(-\varepsilon, \varepsilon)$ .

The origin is asymptotically stable, the other fixed point is unstable.

(ii) If  $0 < \alpha < \alpha_2$ , then  $G_\alpha$  has two fixed points, 0 and  $x_{1\alpha} > 0$  in  $(-\varepsilon, \varepsilon)$ .

The origin is unstable, the other fixed point is asymptotically stable.

**Lemma A.3.** (Supercritical pitchfork bifurcation) Let  $G : U \times I \rightarrow \mathbb{R}$  be as in

630 Lemma A.2, except that  $G$  is  $C^r$  with  $r \geq 3$  and  $\frac{\partial^2 G}{\partial x^2}(0, 0) = 0$ . Further, if  $\frac{\partial^3 G}{\partial x^3}(0, 0) < 0$  then there are  $\alpha_1 < 0 < \alpha_2$  and  $\varepsilon > 0$  such that

(i) If  $\alpha_1 < \alpha \leq 0$ , then  $G_\alpha = G(\cdot, \alpha)$  has a unique fixed point,  $x = 0$ , in  $(-\varepsilon, \varepsilon)$ . It is asymptotically stable.

(ii) If  $0 < \alpha < \alpha_2$ , then  $G_\alpha$  has three fixed points in  $(-\varepsilon, \varepsilon)$ . The origin is

635 an unstable fixed point, the two others,  $x_{1\alpha} < 0 < x_{2\alpha}$ , are asymptotically stable.

Note that the case  $\frac{\partial^2 G}{\partial x \partial \alpha}(0, 0) < 0$  is identical to the above after the change

of parameter  $\alpha \rightarrow -\alpha$ . If  $\frac{\partial^3 G}{\partial x^3}(0, 0) > 0$ , it is a so-called subcritical pitchfork bifurcation. Then for  $\alpha < 0$ , there are three fixed points near the origin, but

640 only  $x = 0$  is asymptotically stable. For  $\alpha \geq 0$ , the origin is the unique fixed point near  $x = 0$ , and it is unstable.

## Acknowledgements

This work is supported by the National Natural Science Foundation of China (NSFCs 61772017, 11631201), and by the Fundamental Research Funds for the  
645 Central Universities (GK201901008).

## References

- [1] Ferguson NM, et al, Strategies for containing an emerging influenza pandemic in southeast asia, *Nature* 437 (2005) 209–214.
- [2] Fraser C, et al, Pandemic potential of a strain of influenza A (H1N1): Early  
650 findings, *Science* 324 (2009) 1557–1561.
- [3] Tang SY, Xiao YN, Yuan L, Cheke RA, Wu JH, Campus quarantine (fengxiao) for curbing emergent infectious diseases: Lessons from mitigating A/H1N1 in Xian, China, *J Theor Biol* 295 (2012) 47–58.
- [4] Xiao YN, Tang SY, Wu JH, Media impact switching surface during an infectious disease outbreak, *Sci Rep* 5 (2015) 7838. doi:10.1038/srep07838.  
655
- [5] Agur Z, Cojocaru L, Mazor G, Anderson RM, Danon YL, Pulse mass measles vaccination across age cohorts, *Proceedings of the National Academy of Sciences of the United States of America* 90 (24) (1993) 11698–11702.
- [6] Mailleret L, Lemesle V, A note on semi-discrete modelling in the life sciences, *Phil Trans R Soc A* 367 (2009) 4779–4799.  
660
- [7] Shulgin B, Stone L, Agur Z, Pulse vaccination strategy in the SIR epidemic model, *Bull Math Biol* 60 (1998) 1123–1148.
- [8] Fuhrman KM, Lauko IG, Pinter GA, Asymptotic behavior of an SI epidemic model with pulse removal, *Math Comput Model* 40 (2004) 371–386.
- [9] Gao SJ, Chen L, Nieto JJ, Torres A, Analysis of a delayed epidemic model with pulse vaccination and saturation incidence, *Vaccine* 24 (2006) 6037–6045.  
665

- [10] Gao SJ, Chen LS, Teng ZD, Impulsive vaccination of an SEIRS model with time delay and varying total population size, Bull Math Biol 69 (2007) 731–745.
- [11] Liu XN, Takeuchi Y, Iwami S, SVIR epidemic models with vaccination strategies, J Theor Biol 253 (2008b) 1–11.
- [12] Meng XZ, Chen LS, The dynamics of a new SIR epidemic model concerning pulse vaccination strategy, Appl Math Comput 197 (2008) 582–597.
- [13] D’Onofrio A, Stability properties of pulse vaccination strategy in SEIR epidemic model, Math Biosci 179 (2002) 57–72.
- [14] D’Onofrio A, On pulse vaccination strategy in the SIR epidemic model with vertical transmission, Appl Math Lett 18 (2005) 729–732.
- [15] Lakmeche A, Arino O, Bifurcation of non-trivial periodic solutions of impulsive differential equations arising chemotherapeutic treatment, Dyn Contin Discret Impul Syst 7 (2000) 265–287.
- [16] Lakmeche A, Arino O, Nonlinear mathematical model of pulsed-therapy of heterogeneous tumors, Nonlinear Anal: Real World Appl 2 (2001) 455–465.
- [17] Panetta JC, A mathematical model of periodically pulsed chemotherapy: tumor recurrence and metastasis in a competitive environment, Bull Math Biol 58 (1996) 425–447.
- [18] Panetta JC, A mathematical model of drug resistance: heterogeneous tumors, Math Biosci 147 (1998) 41–61.
- [19] Bunimovich-Mendrazitsky, Svetlana, Byrne, Helen, Stone, Lewi, Mathematical model of pulsed immunotherapy for superficial bladder cancer, Bull Math Biol 70 (7) (2008) 2055–2076.
- [20] Liu MX, Jin Z, The effect of impulsive control strategy in HIV/AIDS model, Dyn Cont Disc Ser A 13 (2006) 706–713.

- 695 [21] Smith? RJ, Schwartz EJ, Predicting the potential impact of a cytotoxic  
T-lymphocyte hiv vaccine: how often should you vaccinate and how strong  
should the vaccine be, *Math Biosci* 212 (2008) 180–187.
- [22] Bainov DD, Simeonov PS, *Systems with impulsive effect: Stability, Theory  
and Applications*. Wiley, New York.
- [23] Benchohra M, Henderson J, Ntouyas S, *Impulsive differential equations and  
inclusions*, Hindawi Publishing Corporation, New York.
- 700 [24] Kaul SK, On impulsive semidynamical systems, *J Math Anal Appl* 150  
(1990) 120–128.
- [25] Kaul SK, On impulsive semidynamical systems III: Lyapunov stability. re-  
cent trends in differential equations, *Ser Appl Anal* 1 (1992) 335–345.
- 705 [26] Kaul SK, Stability and asymptotic stability in impulsive semidynamical  
systems, *J Applied Math Stochastic Anal* 7 (1994) 509–523.
- [27] Tang SY, Cheke RA, Stage-dependent impulsive models of integrated pest  
management (IPM) strategies and their dynamic consequences, *J Math  
Biol* 50 (2005) 257–292.
- 710 [28] Tang SY, Xiao YN, Chen LS, Cheke RA, Integrated pest management  
models and their dynamical behaviour, *Bull Math Biol* 67 (2005) 115–135.
- [29] Tang SY, Pang WH, Cheke RA, Wu JH, Global dynamics of a state-  
dependent feedback control system, *Adv Diff Equ* 2015 (2015) 322. doi:  
10.1186/s13662-015-0661-x.
- 715 [30] Tang SY, Tang B, Wang AL, Xiao YN, Holling II predator-prey impul-  
sive semi-dynamic model with complex poincare map, *Nonlin Dyndoi*:  
10.1007/s11071-015-2092-3.
- [31] Tang SY, Pang WH, On the continuity of the function describing the times  
of meeting impulsive set and its application, *Math Biosci Eng* 14 (2017)  
720 1399–1406.

- [32] Liang JH, Tang SY, Nieto JJ, Cheke RA, Analytical methods for detecting pesticide switches with evolution of pesticide resistance, *Math Biosci* 245 (2013) 249–257.
- [33] Nie LF, Teng ZD, Hu L, The dynamics of a chemostat model with state dependent impulsive effects, *Int J Bif Chaos* 21 (2011) 1311–1322.
- [34] Tang SY, Chen LS, Modelling and analysis of integrated pest management strategy, *Discrete Contin Dyn Syst B* 4 (2004) 759–768.
- [35] Tang SY, Cheke RA, Models for integrated pest control and their biological implications, *Math Biosci* 215 (2008) 115–125.
- [36] Tang SY, Xiao YN, Cheke RA, Multiple attractors of host-parasitoid models with integrated pest management strategies: Eradication, persistence and outbreak, *Theor Popul Biol* 73 (2008) 181–197.
- [37] Tang SY, Liang JH, Tan YS, Cheke RA, Threshold conditions for integrated pest management models with pesticides that have residual effects, *J Math Biol* 66 (2013) 1–35.
- [38] Zhang Q, Tang B, Tang SY, Vaccination threshold size and backward bifurcation of SIR model with state-dependent pulse control, *J Theor Biol* 455 (2018) 75–85.
- [39] Calabrese EJ, Edward J, Hormesis: changing view of the dose-response, a personal account of the history and current status, *Mutat Res* 511 (3) (2002) 181–189.
- [40] Calabrese EJ, Baldwin LA, Toxicology rethinks its central belief, *Nature* 421 (2003) 691–692.
- [41] Pearce OMT, et al, Inverse hormesis of cancer growth mediated by narrow ranges of tumor-directed antibodies, *Proc Natl Acad Sci USA* 111 (2014) 5998–6003.